Letters in Drug Design & Discovery 22 (2025) 100367

Contents lists available at ScienceDirect

Letters in Drug Design & Discovery

journal homepage: www.keaipublishing.com/en/journals/lddd/

Indole ring linked thiazolidone hybrid molecules as potent tubulin inhibitors

Abdulrahman Abba[a], Naz Unal[b], Zulal Sevgi Dede[b], Ipek Bedir[c], Dilek Telci[c], Başak Aru[d], Gülderen Yanıkkaya Demirel[d], Güneş Yıldırım Akdeniz[e], Ahmet Can Timuçin[f], Burcin Gungor[b], Hülya Akgün[a,*]

[a] Dept. of Pharmaceutical Chemistry, Faculty of Pharmacy, Yeditepe University, Kayışdağı caddesi, Ataşehir, İstanbul, Türkiye
[b] Dept. of Biochemistry, Faculty of Pharmacy, Yeditepe University, Kayışdağı caddesi, Ataşehir, İstanbul, Türkiye
[c] Dept. of Genetics and Bioengineering, Faculty of Engineering, Yeditepe University, Kayışdağı caddesi, Ataşehir, İstanbul, Türkiye
[d] Dept. of Immunology, Faculty of Medicine, Yeditepe University, Kayışdağı caddesi, Ataşehir, İstanbul, Türkiye
[e] Dept. of Molecular Biology, Genetics and Bioengineering, Faculty of Engineering and Natural Sciences, Sabancı University, Tuzla, İstanbul, Türkiye
[f] Dept. of Molecular Biology and Genetics, Faculty of Engineering and Natural Sciences, Acıbadem Mehmet Ali Aydınlar University, Ataşehir, İstanbul, Türkiye

ARTICLE INFO

Keywords:
Indole
Thiazolidin-4-one
Tubulin polymerization inhibitors
Anticancer
Apoptosis
Molecular docking

ABSTRACT

Background: Tubulin inhibitors are a prominent class of antineoplastic agents for cancer therapy, with many established drugs originating from plant-derived compounds such as vinca alkaloids and taxanes.

Method: A new series of twenty-four 5-(substituted) benzylidene-2-{[2-(3H-indol-3-yl)ethyl] imino}-3-phenyl-1,3-thiazolidin-4-one derivatives (1 − 24) was synthesized based on assuming that it would inhibit tubulin polymerization, successfully. To assess their biological potential these derivatives were subjected to a comprehensive screening including cytotoxic activity using various cancer cell lines, cell death studies, cell motility and migration analysis, assessment of the compounds' ability to inhibit tubulin polymerization, and computational analysis.

Results: Out of the twenty-four synthesized compounds, specifically compounds 8, 10, 15, 21, and 23 demonstrated a desirable selective cytotoxic effect against the MCF7 cancer cell line compared to the healthy epithelial counterparts. Mechanistic studies confirmed that these five active compounds functioned as tubulin polymerization inhibitors, exhibiting an inhibitory mechanism similar to that of vinblastine. Computational analyses strongly supported these findings, demonstrating that the five active compounds possessed a high affinity binding to the tubulin structure. Compound 15 was identified as the most potent derivative, causing significant cell cycle arrest and inducing a distinct apoptotic effect in MCF7 cells.

Conclusion: 2-{[2-(3H-indol-3-yl)ethyl]imino}-3-phenyl-5-[(3-hydroxy-4-methoxy phenyl)methylidene]-1,3-thiazolidin-4-one (15) represents a novel chemical series targeting microtubules. This compound emerged as a promising potential hit molecule due to its selective cytotoxicity against MCF7 cells, potent vinblastine-like tubulin polymerization inhibition.

* Corresponding author.
E-mail address: hakgun@yeditepe.edu.tr (H. Akgün).

https://doi.org/10.1016/j.lddd.2026.100367
Received 28 November 2025; Received in revised form 24 December 2025; Accepted 30 December 2025
Available online 6 March 2026
1570-1808/© 2026 Publishing services by Elsevier B.V. on behalf of KeAi Communications Co. Ltd. This is an open access article under the CC BY-NC-ND license (http://creativecommons.org/licenses/by-nc-nd/4.0/).

1. Introduction

Investigating microtubule polymerization as a therapeutic target remains a prominent area of focus in cancer research. Microtubules are considered vital protein polymers that are found in the eukaryotic cells and are essential in preserving cell shape, transporting a variety of cellular components, promoting cell signaling, and enabling cell division and mitosis.[1,2] Many microtubule-targeting molecules, such as Taxanes, Vinca alkaloids, and colchicine are plant-oriented and have been used in cancer treatments.[2,3] However, the complicated chemical structures and limited access to the natural resources, in combination with the development of drug resistance pushed the scientist to develop small organic molecules as microtubule-targeting agents.[4,5]

The indole heterocyclic ring system represents a highly significant privileged structure within the domain of synthetic medicinal chemistry, particularly in the part of structure of the Vinca alkaloids. Specifically, the Vinca alkaloids exert their cytotoxic effect by inhibiting the dynamic polymerization of tubulin monomers into functional microtubules. This disruption of the mitotic spindle apparatus leads to mitotic arrest and ultimately, programmed cell death in proliferating cells. Consequently, this distinct mode of action against cellular division renders the indole-containing scaffolds a profoundly valuable template for the rational design and synthesis of novel chemotherapeutic agents specifically in oncology.[6] So far, many molecules containing the indole nucleus are approved by the FDA as kinase inhibitors, effecting inhibition of VEGFR, and reduces tumor vascularization and causes cell apoptosis. A number of indole derivatives used in cancer chemotherapy[7,8] and many more are currently undergoing clinical evaluation as well. Some of the representatives are depicted in Fig. 1.

Similarly, the thiazolidine ring systems are known to be crucial structural units in drug discovery due to its remarkable activity,[9,10] such as antibacterial,[10,11] antitubercular,[12] anticancer,[13,14] antiviral,[15,16] anti-inflammatory[17] and α- Glucosidase and α-

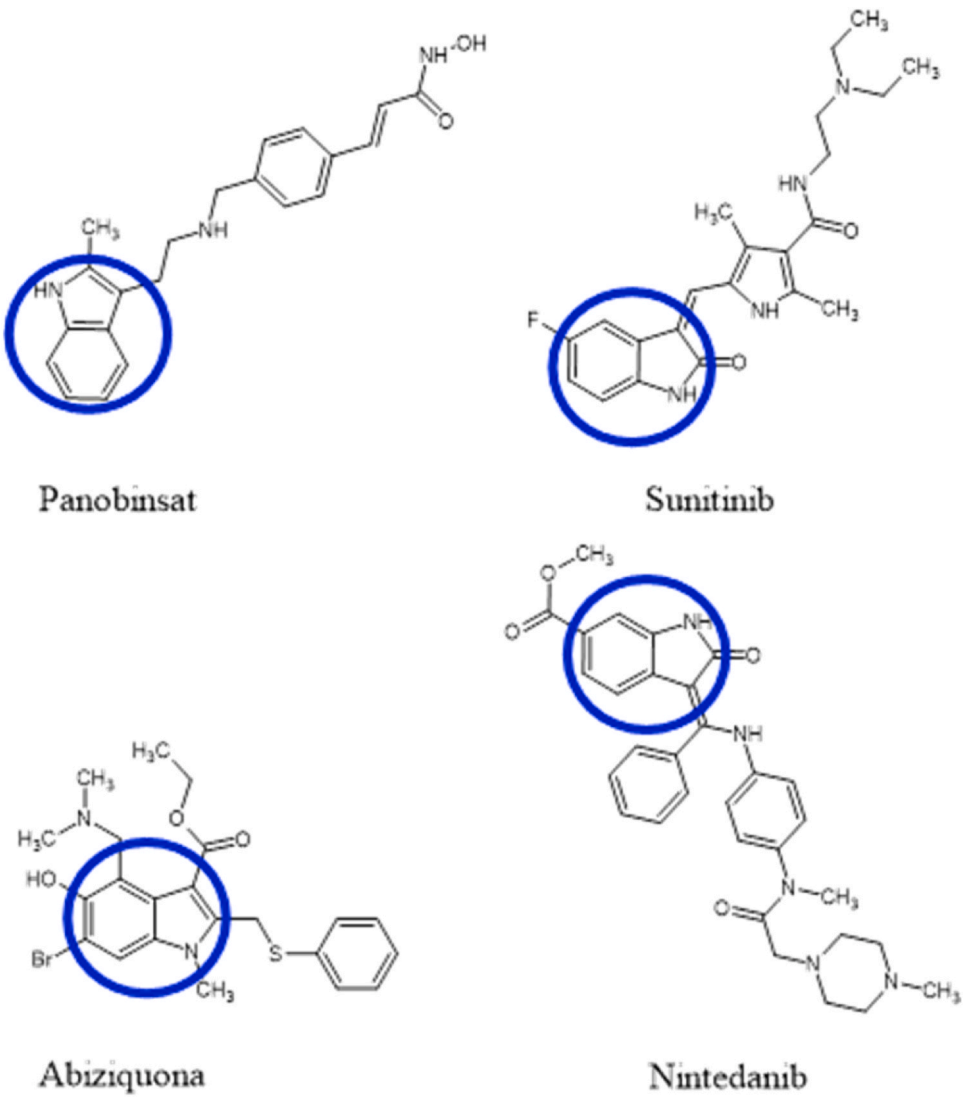

Fig. 1. Some indole derivatives used in cancer therapy in clinic.

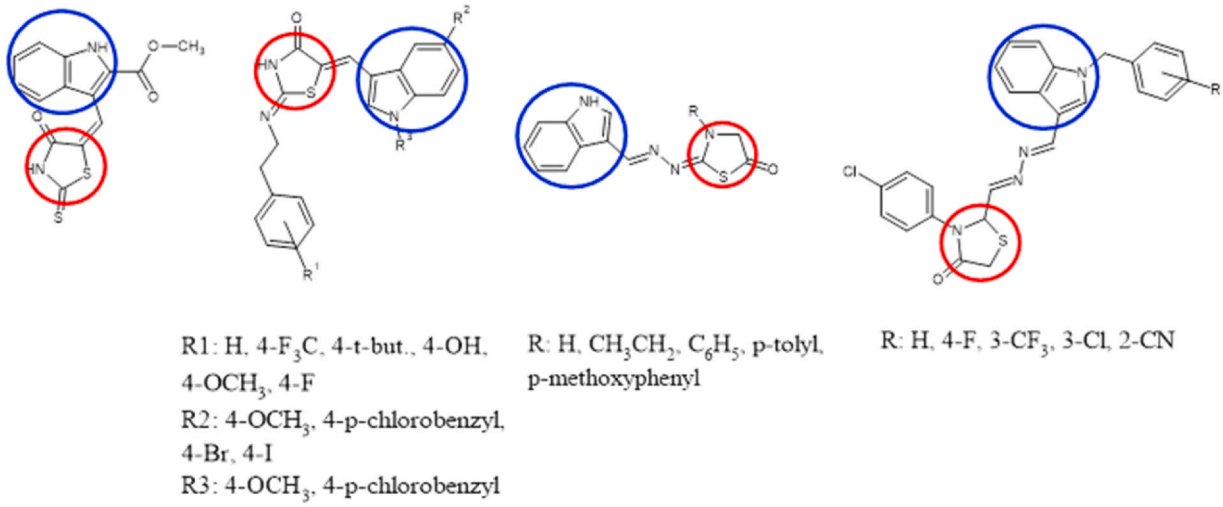

Fig. 2. The structure of representative 4-thiazolidinone moiety with indole ring.

Amylase inhibitory activities[18–20] and Alzheimer's.[21] 5-Benzylidene 2–4-thiazolidinone derivatives reported as antitumor on leukemia and prostate cancer cell lines via the mechanism of kinase inhibitors.[22]

Molecular hybridization is an efficient and often used approach to find novel and active molecules in medicinal chemistry. In recent studies, a combination of the thiazolidinone ring with indole has been suggested as a promising hybrid scaffold for the new anti-cancer drug-like compounds.[19,23] The hybrid scaffold formed by integrating the 4-thiazolidinone and indole rings into a single molecule, as illustrated in Fig. 2.[24,25]

In the light of above-mentioned findings, new hybrid molecules, 5-(substituted)benzylidene-2-{[2-(3H-indol-3-yl)ethyl]imino}-3-phenyl-1,3-thiazolidin-4-one's (1 − 24) were synthesized and evaluated for their cytotoxic activity against five human cancer cell lines: MCF7 (breast cancer), MCF12A (mammary epithelial), HUVEC (endothelial), A549 (lung cancer) and PC3 (prostate adenocarcinoma). Mechanistic studies demonstrated that the compounds possess tubulin inhibitory activity, which is in line with their apoptotic effects. Furthermore, a computational study was conducted involving molecular docking analyses at the vinblastine binding site of the tubulin dimer.

2. Materials and methods

2.1. Chemistry

2.1.1. General experimental methods

All the reagents and solvents were purchased from Sigma Aldrich. Melting points (°C) determination of compounds were done by using a Mettler Toledo FP62 capillary melting point apparatus and were uncorrected. All compounds except compounds 1–8 were purified by column chromatography using silica gel (60 mesh) as stationary phase and hexane: ethyl acetate (60:40) solution and chloroform: methanol (90:10) as mobile phases. Column was filled according to wet method. Elution was controlled with TLC (thin layer chromatography) using silica gel plates. TLC aluminum sheets 20 × 20 cm silica gel 60 F254 (Merck) were used as stationary phase, and preparation of two different solvent systems which are hexane: ethyl acetate (60:40) and chloroform: methanol (90:10). Infrared spectra were collected on a Perkin-Elmer Spectrum One series FT-IR apparatus (Version 5.0.1), by applying potassium bromide (KBr) as a background, and the frequencies were shown in cm-1. 1H-NMR and 13C-NMR spectra were collected with a Varian Mercury-400 FT NMR spectrometer (Varian Inc., Palo Alto, CA USA) by applying of tetramethyl silane (TMS) as the internal reference, with deuterated dimethyl sulfoxide (DMSO-d6) or deuterated chloroform (CDCl3) as a solvent, and the chemical shifts were reported in parts per million (ppm). LC/MS spectra were recorded via Revident LC/Q-TOF.

2.2. Method of synthesis

2.2.1. Synthesis of 1-(2-(indole-3-yl) ethyl)-3-phenylthiourea (I)

10 mmol (1 mL) of phenylisothiocyanate was dissolved in 10 mL toluene and placed in a round bottom flask then 8.3 mmol (1.33 g) tryptamine was added to this mixture and stirred at room temperature. Reaction was monitored by TLC with silica gel plate and hexane: ethyl acetate (6:4) and chloroform: methanol (90:10) mobile phases. After a while white precipitation started to appear. Stirring was continued for 2 h. The precipitated crude product was collected by filtration, washed several times with toluene, and dried to afford the final product to yield 74% of pure product 1.

2.2.2. Synthesis of 2-{[2-(3H-indol-3-yl)ethyl]imino}-3-phenyl-1,3- thiazolidin-4-one (II)

1.7 mmol (0.5 g) of 1-(2-(indole-3-yl) ethyl)-3-phenylthiourea was dissolved in 2.5 mL ethanol, then 3.4 mmol (0.28 g) anhydrous sodium acetate was added to this mixture. The resulting mixture was maintained under cold conditions, and subsequently 4.25 mmol (0.34 g) of chloroacetyl chloride was added. The reaction was seemed to complete after 12 h of constant stirring during reflux. The progress of the reaction was monitored using TLC with a silica gel plate and a hexane: ethyl acetate (6:4) and chloroform: methanol (90:10) mobile phases. To facilitate the precipitation of the product, the reaction mixture was cooled overnight in a freezer. The resulting solid product was then collected via filtration and washed with ice-cold ethanol to yield a pure product to yield 71% of pure product 1.

2.2.3. Synthesis of 5-(substituted) benzylidene-2-{[2-(3H-indol-3-yl) ethyl] imino}-3-phenyl-1,3-thiazolidin-4-one (III)

1.5 mmol (0.5 g) of (2E/Z)-2-{[2-(3H-indol-3-yl)ethyl]imino}-3-phenyl-1,3- thiazolidin-4-one and 3 mmol (0.30 mL) of piperidine were dissolved in 2.5 mL ethanol then 4.5 mmol of different aromatic aldehyde derivatives were added dropwise onto this mixture. The reactions were allowed to proceed under constant stirring and reflux conditions for 30 h. The progress of the reactions was monitored using TLC with a silica gel plate and a hexane: ethyl acetate (6:4) and chloroform: methanol (90:10) mobile phases mixture. If no precipitation was observed, the mixture was cooled in the freezer to facilitate precipitation. The resulting precipitates were filtered and isolated using either recrystallization from appropriate solvents or column chromatography with suitable mobile phase systems to yield 20–81% of products differing for each substituent presented 1.

2.2.4. 5-benzylidene-2-{[2-(3H-indol-3-yl)ethyl]imino}-3-phenyl-1,3-thiazolidin-4-one 1

1.5 mmol (0.5 g) of II, 4.5 mmol benzaldehyde (0.045 mL) and 3 mmol (0.30 mL) of piperidine were reacted in 2.5 mL of ethanol as described in general procedure III and recrystallized from ethanol to as yellowish powder with a yield 47% (0.297 g), mp 161.2 ˚C; FT-IR (νmax (KBr, cm-1): 3391 (N-H), 3027–3076 (aromatic C═C-H), 2924 (aliphatic C-H), 1707 (C═O), 1635 (aromatic C═C), 1140 (C-N); 1H-NMR (400 MHz, $CDCl_3$): δ/ppm = 3.3/ppm (2 H, CH2 t, J = 6.9 Hz), 4.30 (2 H, CH_2 t, J = 6.9 Hz), 6.91 (2 H, d, aromatic), 7.17 (4 H, m, aromatic), 7.62 (9 H, m, aromatic), 7.8 (1 H, s, Ar- CH), 8.1 (1 H, NH s); LC/Q-TOF *m/z* 423.140 Anal. Calcd for $C_{26}H_{21}N_3OS$: M + : 423.139984, M: 423.14053, [M + H] + : 424.147809; Found: *m/z*: M + 423.13998, M: 423.14053, [M + H] + : 424.14781.

2.2.5. 2-{[2-(3H-indol-3-yl)ethyl]imino}-3-phenyl-5-[(4-nitrophenyl)methylidene]-1,3-thiazolidin-4-one 2

1.5 mmol (0.5 g) of II, 4.5 mmol nitro benzaldehyde (0.045 mL) and 3 mmol (0.30 mL) of piperidine were reacted in 2.5 mL of ethanol as described in general procedure III and recrystallized from 95% ethanol with a 48% yield, mp 242 oC; FT-IR νmax (KBr, cm-1) 3441 (N-H), 3045–3077 (aromatic C═C-H), 2982 (aliphatic C-H), 1708, (C═O), 1592–1607 (aromatic C═C), 1243 (C-N); 1H-NMR (400 MHz, $CDCl_3$): δ/ppm = 3.16 (2 H, CH_2 t, J = 6.9 Hz), 4.20 (2 H, CH_2 t, J = 6.9 Hz),6. 91 (4 H, m, aromatic), 7.17 (5 H, m, aromatic), 7.62 (1 H, m, aromatic), 7.88 (H, s, Ar- CH), 8.22 (1 H, m, aromatic), 8.39 (2 H, m, aromatic), 10.80 (1 H, NH s); ^{13}C NMR (400 MHz, DMSO-d6) δ/ppm = 23.18, 44.1, 110.8, 111.9, 118.6, 118.9, 121.3, 121.5, 123.6, 124.8, 125.5, 126.2, 127.7, 128.0, 130.0, 131.2, 136.7, 140.1, 147.6, 148.1, 149.3, 165.8; LC/Q-TOF *m/z* 469.140 Anal. Calculd for $C_{26}H_{21}N_4O_3S$: M + : 469.132338, M: 469.13344, [M + H] + : 470.140163. Found: *m/z*: M + : 469.13289, M: 469.13344, [M + H] + : 470.14071.

2.2.6. 2-{[2-(3H-indol-3-yl)ethyl]imino}-3-phenyl-5-[(4-chlorophenyl)methylidene]-1,3-thiazolidin-4-one 3

1.5 mmol (0.5 g) of II, 4.5 mmol 4-chloro benzaldehyde (0.045 mL) and 3 mmol (0.30 mL) of piperidine were reacted in 2.5 mL of ethanol as described in general procedure III and recrystallized from 95% ethanol with a 4% yield as yellowish powder, mp 220.1 ˚C; FT-IR νmax (KBr, cm-1) 3396 (N-H), 3056 (aromatic C═C-H), 2942 (aliphatic C-H), 1708 (C═O), 1590–1612 (aromatic C═C), 1240 (C-N); ^{1}H NMR (400 MHz, $CDCl_3$): δ/ppm = 3.17 (2 H, t, CH2 J = 7.2 Hz), 4.31 (2 H, t, CH_2, J = 7.2 Hz, 6.91 (2 H, m, aromatic), 7.10–7.25 (4 H, m, aromatic), 7.30–7.45 (7 H, m, aromatic), 7.8 (1 H, s, Ar-CH), 7.85 (1 H, d, aromatic), 8.01 (1 H, NH s); ^{13}C NMR (400 MHz, DMSO-d6) δ/ppm = 23.21, 43.93, 110.92, 111.91, 118.60, 118.87, 121.37, 121.49, 122.51, 123.60, 125.33, 127.70, 129.25, 129.81, 129.96, 131.89, 132.67, 134.97, 136.73, 148.28, 149.73, 166.05; LC/Q-TOF *m/z* 457.101 Anal. Calcd. for $C_{20}H_{20}ClN_3OS$: M + : 457.101011, M: 457.10156, [M + H] + : 458.108836; Found: *m/z*: M + : 457.10101, M: 457.10156, [M + H] + : 458.10884

2.2.7. 2-{[2-(3H-indol-3-yl)ethyl]imino}-3-phenyl-5-[(3-methylphenyl)methylidene-1,3-thiazolidin-4-one 4

1.5 mmol (0.5 g) of II, 4.5 mmol (0.5407 g) of 3-methyl benzaldehyde and 3 mmol (0.30 mL) of piperidine were reacted in 2.5 mL of ethanol with as described in general procedure III and recrystallized from 95% ethanol with a 43% yield as yellow powder, mp: 177.1 (˚C); FT-IR νmax (KBr, cm-1): 3402 (N-H), 3057–3109 (aromatic C═C-H), 2943 (aliphatic C-H), 1709, (C═O), 1594–1639 (aromatic C═C), 1283 (C-N); 1 H NMR (400 MHz, $CDCl_3$): δ/ppm = 2.36 (3 H, CH3, s), 3.26 (2 H, t, CH2, J = 7.2 Hz), 4.29 (2 H, t, CH_2, J = 7.2 Hz), 6.91 (2 H, m, aromatic), 7.10–7.45 (8 H, m, aromatic), 7.50 (3 H, m, aromatic), 7.8 (1 H, s, Ar-CH), 7.85 (1 H, d, aromatic), 8.01 (1 H, NH s); LC/Q-TOF *m/z* 437.56 Anal. Calcd. for $C_{27}H_{23}N_3OS$ M + : 437.155634, M: 437.15618, [M + H] + : 438.163459; Found: *m/z*: M + : 437.15563, M: 437.15618, [M + H] + : 438.16346.

2.2.8. 2-{[2-(3H-indol-3-yl)ethyl]imino}-3-phenyl-5-[(3methxoyphenyl)methylidene]-1,3-thiazolidin-4-one 5

1.5 mmol (0.5 g) of II, 4.5 mmol (0.5475 g) of 3-methoxy benzaldehyde and 3 mmol (0.30 mL) of piperidine were reacted in 2.5 mL of ethanol as described in general procedure III and recrystallized from 95% ethanol with a 31% yield as yellow solid. mp 163 ˚C; FT-IR νmax (KBr, cm-1): 3401 (N-H), 3057–3075 (aromatic C═C-H), 2945 (aliphatic C-H), 1709, (C═O), 1594–1612 (aromatic

C═C), 1242 (C-N); 1H-NMR (400 MHz, CDCl3): δ/ppm = 3.1 (2 H, CH_2, s), 3.7 (3 H, t, CH_3 J = 7.2 Hz), 4.20 (2 H, t, CH_2, J = 7.2 Hz), 6.92–6.94 (6 H, m, aromatic), 7.10–7.45 (6 H, m, aromatic), 7.50 (1 H, m, aromatic), 7.80 (1 H, s, Ar-CH), 7.85 (1 H, d, aromatic), 10.9 (1 H, NH, s); LC/Q-TOF *m/z* 453.151 Anal. Calcd. for $C_{27}H_{23}N_3O_2S$: M + : 453.150548, M + : 453.15110, [M + H] + : 454.158373; Found *m/z*: M + : 453.15055, M: 453.1511, [M + H] + : 454.15837.

2.2.9. 2-{[2-(3H-indol-3-yl)ethyl]imino}-3-phenyl-5-[(2-ethylphenyl) methylidene]-1,3-thiazolidin-4-one 6

1.5 mmol (0.5 g) of II, 4.5 mmol (0.5919 mL) of 2-ethyl benzaldehyde and 3 mmol (0.30 mL) of piperidine were reacted in 2.5 mL of ethanol as described in general procedure III and recrystallized from 95% ethanol with a 28% yield as yellow solid. mp 170.1 ˚C; FT-IR νmax (KBr, cm-1): 3401 (N-H), 3057–3075 (aromatic C═C-H), 2946 (aliphatic C-H), 1710, (C═O), 1594–1612 (aromatic C═C), 1242 (C-N); ^{1}H NMR (400 MHz, $CDCl_3$): δ/ppm = 1.5 (3 H, CH_3, t, J = 7.2 Hz), 2.8 (2 H, CH_2, q, J = 7.2 Hz), 3.4 (3 H, t, CH_3 J = 7.2 Hz), 4.20 (2 H, t, CH_2, J = 7.2 Hz), 6.92–6.94 (2 H, m, aromatic), 7.10–7.45 (7 H, m, aromatic), 7.50 (4 H, m, aromatic), 7.8 (1 H, s, Ar-CH), 7.9 (1 H, NH, s). 8.1 (2 H, d, aromatic); ^{13}C NMR ppm (400 MHz, DMSO-d6) δ/ppm = 16.03, 23.25, 26.40, 43.89, 111.00, 111.91, 118.57, 118.87, 121.36, 121.48, 123.61, 123.81, 125.24, 127.08, 127.71, 128.26, 129.84, 129.88, 130.54, 132.23, 136.75, 144.59, 148.39, 150.37, 165.91; LC/Q-TOF *m/z* 451.171 Anal. Calcd. for $C_{28}H_{25}N_3OS$: M + : 451.171284, M: 451.17183, [M + H] + : 452.179109. Found: *m/z*: M + : 451.17128, M: 451.17183, [M + H] + : 452.171911.

2.2.10. 2-{[2-(3H-indol-3-yl)ethyl]imino}-3-phenyl-5-[(2-methylphenyl)methylidene]-1,3-thiazolidin-4-one 7

1.5 mmol (0.5 g) of II, 4.5 mmol (0.5407 g) of 2-methyl benzaldehyde and 3 mmol (0.30 mL) of piperidine were reacted in 2.5 mL of ethanol as described in general procedure III and recrystallized from 95% ethanol with a 24% yield as yellow solid, mp:167 ˚C; FT-IR νmax (KBr, cm-1) 3445 (N-H), 3013–3056 (aromatic C═C-H), 2956 (aliphatic C-H), 1697(C═O), 1590–1606 (aromatic C═C), 1229 (C-N); ^{1}H NMR (400 MHz, $CDCl_3$): δ/ppm = 2.5 (3 H, s, CH_3), 3.33 (2 H, CH_2 t, J = 6.9 Hz), 4.35 (2 H, CH_2 t, J = 6.9 Hz), 6.91 (2 H, m, aromatic), 7.17 (7 H, m, aromatic), 7.62 (4 H, m, aromatic), 7.8 (1 H, s, Ar-CH), 7.99 (1 H, d, aromatic), 8.1 (1 H, NH, s); ^{13}C NMR (400 MHz, DMSO-d6) δ/ppm = 19.86, 23.26, 43.84, 110.92, 111.94, 118.57, 118.84, 121.37,121.45, 123.47, 123.60, 125.26, 127.05, 127.49, 127.70, 128.41, 129.90, 130.36, 131.33,132.91, 136.76, 138.70, 148.37, 150.34, 165.93; LC/Q-TOF *m/z* 437.156 Anal. Calcd. for $C_{27}H_{23}N_3OS$: *m/z*: M + : 437.155634, M: 437.15618, [M + H] + : 438.163459. Found: *m/z*: M + : 437.15563, M: 437.15618, [M + H] + : 438.16346.

2.2.11. 2-{[2-(3H-indol-3-yl)ethyl]imino}-3-phenyl-5-[(4-hydoxyphenyl)methylidene]-1,3-thiazolidin-4-one 8

1.5 mmol (0.5 g) of II,.5 mmol (0.5495 g) of 4-hydroxy benzaldehyde and 3 mmol (0.30 mL) of piperidine in 2.5 mL of ethanol were reacted as described in general procedure III and recrystallized from 95% ethanol with a 28% yield as brown-orange solid, mp:236˚C; FT-IR νmax (KBr, cm-1) 3429 (N-H), 3381 (OH), 3052–3163 (aromatic C═C-H), 2962 (aliphatic C-H), 1684 (C═O), 1584–1630 (aromatic C═C), 1257 (C-N); 1H-NMR (400 MHz, $CDCl_3$): δ/ppm_ 3.5 (2 H, t, CH_2, J = 7.1 Hz), 4.1 (2 H, CH_2 t, J = 6.9 Hz), 6.91 (4 H, m, aromatic), 7.17 (1 H, m, aromatic), 7.40 (2 H, m, aromatic), 7.60 (4 H, m, aromatic), 7.8 (1 H, s, Ar-CH), 7.90 (3 H, d, aromatic), 8.1 (1 H, NH, s); ^{13}C NMR (400 MHz, DMSO-d6) δ/ppm = 23.26, 43.71, 111.03, 111.89, 116.77, 117.19, 118.64, 118.86, 121.44, 121.48, 123.54, 124.65, 125.13, 127.73, 129.92, 131.09, 132.55, 136.74, 148.55, 150.38, 160.06, 166.46; LC/Q-TOF *m/z* 439.135 Anal. Calcd. for $C_{26}H_{21}N_3O_2S$: *m/z*: M + : 439.134898, M: 439.13545, [M + H] + : 440.142723; Found: *m/z*: M + : 439.1349, M: 439.13545, [M + H] + : 440.14272.

2.2.12. 2-{[2-(3H-indol-3-yl)ethyl]imino}-3-phenyl-5-[(3-fluorophenyl)methylidene]-1,3-thiazolidin-4-one 9

1.5 mmol (0.5 g) of II, 4.5 mmol (0.4773 mL) of 3-fluoro benzaldehyde and 3 mmol (0.30 mL) of piperidine were reacted in 2.5 mL of ethanol as describe in general procedure III and recrystallized from 95% ethanol with a 50% yield as yellow solid, mp:163˚C; FT-IR νmax (KBr, cm-1) 3396 (N-H), 3056 (aromatic C═C-H), 2942 (aliphatic C-H), 1708 (C═O), 1590–1612 (aromatic C═C), 1240 (C-N); 1H-NMR (400 MHz, $CDCl_3$): δ/ppm = 3.5 (2 H, t, CH_2 J = 7.1 Hz), 4.5 (2 H, CH_2 t, J = 6.9 Hz), 6.91 (2 H, m, aromatic), 7.17 (1 H, m, aromatic), 7.22 (3 H, m, aromatic), 7.40 (4 H, d, aromatic), 7.55 (4 H, d, aromatic), 7.8 (1 H, s, Ar-CH), 8.1 (1 H, NH); LC/Q-TOF *m/z* 441.131 Anal. Calcd. for $C_{26}H_{20}FN_3OS$: *m/z*: M + : 441.130562, M: 441.13111, [M + H] + : 442.138387; Found: *m/z*: M + : 441.13056, M: 441.13111, [M + H] + : 442.13839.

2.2.13. {[2-(3H-indol-3-yl)ethyl]imino}-3-phenyl-5-[(3-ethoxy-hydroxyphenyl)methylidene]-1,3-thiazolidin-4-one 10

1.5 mmol (0.5 g) of II, 4.5 mmol (0.7478 g) 4-hydroxy-3-ethoxy benzaldehyde and 3 mmol (0.30 mL) of piperidine were reacted in 2.5 mL of ethanol as described in general procedure III and recrystallized from 95% ethanol with a 43% yield as dark yellow solid, mp:175–177˚C; FT-IR νmax (KBr, cm-1): 3397 (N-H), 3515 (OH), 3031–3055 (aromatic C═C-H), 2978 (aliphatic C-H), 1706 (C═O), 1584–1602 (aromatic C═C), 1241 (C-N); ^{1}H-NMR (400 MHz, DMSO-d6):: δ/ppm = 1.31 (3 H, t, CH_2, J = 7.0 Hz), 3.1 (2 H, t, CH_3 J = 7.1 Hz),3.9 (2 H, CH_2, q, J = 6.9 Hz), 4.1 (2 H, CH_2 t, J = 6.9 Hz), 6.91 (5 H, m, aromatic), 7.17 (4 H, m, aromatic), 7.62 (3 H, m, aromatic), 7.8 (1 H, s, Ar-CH), 11.1 (1 H, NH, s); LC/Q-TOF *m/z* 483.161 Anal. Calcd. for $C_{28}H_{25}N_3O_3S$: M + : 483.161113, M: 483.16166, [M + H] + : 484.168938. Found: *m/z*: M + : 483.16111, M: 483.16166, [M + H] + : 484.16894.

2.2.14. 2-{[2-(3H-indol-3-yl)ethyl]imino}-3-phenyl-5-[(2-methxyphenyl)methylidene]-1,3-thiazolidin-4-one 11

1.5 mmol (0.5 g) of II, 4.5 mmol (0.6126 g) of 2-methoxy benzaldehyde and 3 mmol (0.30 mL) of piperidine were reacted in 2.5 mL of ethanol with as described in general procedure III and recrystallized from 95% ethanol with a 48% yield as yellow solid, mp:171˚C; FT-IR νmax (KBr, cm-1): 3356 (N-H), 3029–3045 (aromatic C═C-H), 2998 (aliphatic C-H), 1700 (C═O), 1594 (aromatic C═C), 1250 (C-N); ^{1}H-NMR (400 MHz, DMSO-d6): δ/ppm = 3.1 (2 H, t, CH_2, J = 7.1 Hz), 3.9 (3 H, CH_3, s, J = 6.9 Hz), 4.1 (2 H, CH_2

t, J = 6.9 Hz), 6.91–7.5 (12 H, m, aromatic), 7.8 (1 H, s, Ar-CH), 7.99 (1 H, s, aromatic), 8.1 (1 H, NH, s); LC/Q-TOF *m/z* 453.151 Anal. Calcd. for $C_{27}H_{23}N_3O_2S$: M + : 453.150548, M: 453.15110, [M + H] + : 454.158373, Found: *m/z*: M + : 453.15055, M: 453.1511, [M + H] + : 454.15837.

2.2.15. 2-{[2-(3H-indol-3-yl)ethyl]imino}-3-phenyl-5-[(2,4-dimethoxyphenyl)methyldene]-1,3-thiazolidin-4-one 12

1.5 mmol (0.5 g) of II, 4.5 mmol (0.7478 g) of 2,4-dimethoxy benzaldehyde and 3 mmol (0.30 mL) of piperidine were reacted in 2.5 mL of ethanol as described in the general procedure III and recrystallized from 95% ethanol with a 69% yield as yellow solid, mp:198 ˚C; FT-IR νmax (KBr, cm-1): 3373 (N-H), 3038–3079 (aromatic C═C-H), 2998 (aliphatic C-H), 1686 (C═O), 1586–1625 (aromatic C═C), 1268 (C-N); 1H-NMR (400 MHz, DMSO-d6): δ/ppm = 3.1 (2 H, t, CH_2 J = 7.1 Hz), 3.9 (6 H, OCH_3, s, J = 6.9 Hz), 4.3 (2 H, CH_2 t, J = 6.9 Hz), 6.5 (2 H, m, aromatic), 6.91 (2 H, m, aromatic), 7.17 (4 H, m, aromatic), 7.45 (1 H, d, aromatic), 7.62 (3 H, m, aromatic), 7.8 (1 H, s, Ar-CH), 8.01 (1 H, d, aromatic), 8.2 (1 H, NH, s,); LC/Q-TOF *m/z* 483.161 Anal. Calcd. for $C_{28}H_{25}N_3O_3S$: M + : 483.161113, M: 483.16166, [M + H] + : 484.168938. Found: *m/z*: M + : 483.16111, M: 483.16166, [M + H] + : 484.16894.

2.2.16. 2E/Z,5E/Z)-2-{[2-(3H-indol-3-yl)ethyl]imino}-3-phenyl-5-[(4-bromophenyl) methylidene]-1,3-thiazolidin-4-one 13

1.5 mmol (0.5 g) of II, 4.5 mmol (0.8326 g) of 4-bromo benzaldehyde and 3 mmol (0.30 mL) of piperidine in were reacted in 2.5 mL of ethanol as described in the general procedure III and recrystallized from 95% ethanol with a 20% yield as yellow-orange solid, mp: 218 ˚C; FT-IR νmax (KBr, cm-1): 3354 (N-H), 3029–3077 (aromatic C═C-H), 2953 (aliphatic C-H), 1697(C═O), 1593–1605 (aromatic C═C), 1281 (C-N); ^{1}H-NMR (400 MHz, DMSO- d6): δ/ppm = 3.45 (2 H, t, CH_2 J = 7.1 Hz), 4.3 (2 H, CH_2 t, J = 6.9 Hz), 6.5 (2 H, m, aromatic), 6.91 (1 H, m, aromatic), 7.17 (1 H, m, aromatic), 7.45 (2 H, m, aromatic), 7.62 (5 H, m, aromatic), 7.8 (1 H, s, Ar-CH), 7.88 (3 H, m, aromatic), 11.1 (1 H, NH, s); LC/Q-TOF *m/z* 501.051 Anal. Calcd. for $C_{26}H_{20}BrN_3OS$: M + : 501.050489, M: 501.05105, [M + H] + : 502.058314 Found: *m/z*: M + : 501.0505, M: 501.05105, [M + H] + : 502.05832.

2.2.17. 2-{[2-(3H-indol-3-yl)ethyl]imino}-3-phenyl-5-[(4-fluorophenyl)methylidene]-1,3-thiazolidin-4-one 14

1.5 mmol (0.5 g) of II, 4.5 mmol (0.4827 mL) of 4-fluoro benzaldehyde and 3 mmol (0.30 mL) of piperidine were reacted in 2.5 mL of ethanol as described in the general procedure III and recrystallized from 95% ethanol with a 38% yield as orange solid mp:206 ˚C; FT-IR νmax (KBr, cm-1): 3416 (N-H), 3055 (aromatic C═C-H), 2934 (aliphatic C-H), 1702 (C═O), 1591–1633 (aromatic C═C), 1235 (C-N); 1H NMR (400 MHz, DMSO-d6): δ/ppm = 3.1 (2 H, t, CH_2, J = 7.1 Hz), 4.1 (2 H, CH_2 t, J = 6.9 Hz), 6.5 (6 H, m, aromatic), 6.91 (2 H, m, aromatic), 7.17 (5 H, m, aromatic), 7.45 (1 H, d, aromatic), 7.8 (1 H, s, Ar-CH); LC/Q-TOF *m/z* 441.131 Anal. Calcd. for $C_{26}H_{20}FN_3OS$: M + : 441.130532, M: 441.13111, [M + H] + : 442.138387; Found: *m/z*: M + : 441.13056, M: 441.13111, [M + H] + : 442.13839.

2.2.18. 2-{[2-(3H-indol-3-yl)ethyl]imino}-3-phenyl-5-[(3-hydroxy-4-methoxy phenyl)methylidene]-1,3-thiazolidin-4-one 15

1.5 mmol (0.5 g) of II, 4.5 mmol (0.6846 g) of 3-hydroxy-4-methoxy benzaldehyde and 3 mmol (0.30 mL) of piperidine were reacted in 2.5 mL of ethanol as described in the general procedure III and recrystallized from acetic acid with a 52% yield as light yellow solid, mp:241 ˚C; FT-IR νmax (KBr, cm-1) 3506 (N-H), 3265 (OH), 3017–3577 (aromatic C═C-H), 2944 (aliphatic C-H), 1708 (C═O), 1593–1630 (aromatic C═C), 1249 (C-N); ^{1}H NMR (400 MHz, DMSO-d6): δ/ppm = 3.1 (2 H, t, CH_2, J = 7.1 Hz), 4.3 (2 H, CH_2, t, J = 6.9 Hz), 6.5 (2 H, m, aromatic), 6.91 (2 H, m, aromatic), 7.17 (4 H, m, aromatic), 7.45 (1 H, d, aromatic), 7.62 (3 H, m, aromatic), 7.8 (1 H, s, Ar-CH), 8.01 (1 H, d, aromatic), 8.2 (1 H, NH, 1 s); 13C-NMR δ ppm (400 MHz, DMSO-d6) δ/ppm = 19.03, 23.25, 26.71, 43.73, 46.97, 56.07, 56.50, 111.03,111.90, 112.89, 115.85, 118.29, 118.63, 118.86, 121.45, 121.48, 123.55, 123.82, 125.16,126.48, 127.72, 129.93, 131.06, 136.74, 147.38, 148.54, 150.16, 150.40, 166.39; LC/Q-TOF *m/z* 469.146 Anal. Calcd. for $C_{27}H_{23}N_3O_3S$: M + : 469.145463, M: 469.14601, [M + H] + : 470.153288; Found *m/z*: M + : 469.14546, M: 469.14601, [M + H] + : 470.15329.

2.2.19. 2-{[2-(3H-indol-3-yl)ethyl]imino}-3-phenyl-5-[(2,3-dimethylphenyl)methylidene]-1,3-thiazolidin-4-one 16

1.5 mmol (0.5 g) of II, 4.5 mmol (0.5869 mL) of 2,3-dimethyl benzaldehyde and 3 mmol (0.30 mL) of piperidine were reacted in 2.5 mL of ethanol as described in the general procedure III and recrystallized from 95% ethanol with a 78% yield as yellow solid, mp:196–197 ˚C; FT-IR νmax (KBr, cm-1): 3352 (N-H), 3015–3057 (aromatic C═C-H), 2923 (aliphatic C-H), 1697(C═O), 1596 (aromatic C═C), 1230 (C-N); ^{1}H NMR (400 MHz, DMSO-d6): δ/ppm = 2.4 (6 H, CH_3, s, J = 6.9 Hz), 3.1 (2 H, t, CH_2 J = 7.1 Hz), 4.3 (2 H, CH_2 t, J = 6.9 Hz), 6.5 (2 H, m, aromatic), 6.91 (1 H, m, aromatic), 7.17 (6 H, m, aromatic), 7.45 (3 H, m, aromatic), 7.62 (1 H, m, aromatic), 7.8 (1 H, s, Ar-CH), 11 (1 H, NH, s); LC/Q-TOF *m/z* 451.171 Anal. Calcd. for $C_{28}H_{25}N_3OS$: M + : 451.171284, M: 451.17183, [M + H] + : 452.179109; Found: *m/z*: M + : 451.17128, M: 451.17183, [M + H] + : 452.17911.

2.2.20. 2-{[2-(3H-indol-3-yl)ethyl]imino}-3-phenyl-5-[(2-bromophenyl)methylidene]-1,3-thiazolidin-4-one 17

1.5 mmol (0.5 g) of II, 4.5 mmol (0.5253 mL) of 2-bromo benzaldehyde and 3 mmol (0.30 mL) of piperidine were reacted in 2.5 mL of ethanol as described in the general procedure III and recrystallized from 95% ethanol with a 46% yield as yellow solid, mp:206 ˚C; FT-IR νmax (KBr, cm-1): 3396 (N-H), 3056 (aromatic C═C-H), 2942 (aliphatic C-H), 1708 (C═O), 1590–1612 (aromatic C═C), 1240 (C-N); ^{1}H NMR (400 MHz, DMSO-d6): δ/ppm 3.1 (2 H, t, CH_2 J = 7.1 Hz), 4.1 (2 H, CH_2 t, J = 6.9 Hz), 6.8 (4 H, m, aromatic), 6.91 (2 H, m, aromatic), 7.17 (2 H, m, aromatic), 7.45 (6 H, m, aromatic), 7.62 (2 H, m, aromatic), 7.8 (1 H, s, Ar-CH); LC/Q-TOF *m/z* 501.051 Anal. Calcd. for $C_{26}H_{20}BrN_3OS$: M + : 501.050489, M: 501.05105, [M + H] + : 502.058314; Found: *m/z*: M + : 501.0505, M: 51.05105, [M + H] + : 502.05832.

2.2.21. 2-{[2-(3H-indol-3-yl)ethyl]imino}-3-phenyl-5-[(3-bromo-4-hydroxyphenyl)methylidene]-1,3-thiazolidin-4-one 18

1.5 mmol (0.5 g) of II, 4.5 mmol (0.9046 g) of 3-bromo-4-hydroxy benzaldehyde and 3 mmol (0.30 mL) of piperidine in 2.5 mL of ethanol were reacted as described in the general procedure III and recrystallized from 95% ethanol with a 51% yield as dark yellow solid, mp: 221°C; FT-IR νmax (KBr, cm-1): 3425 (N-H), 3358 (OH), 3031–3083 (aromatic C═C-H), 2946 (aliphatic C-H), 1679 (C═O), 1584 (aromatic C═C), 1279 (C-N); 1H NMR (400 MHz, DMSO-d6)δ/ppm = 3.1 (2 H, t, CH_2 *J* = 7.1 Hz), 4.3 (2 H, CH_2, t, *J* = 6.9 Hz), 6.8 (5 H, m, aromatic), 6.91 (2 H, m, aromatic), 7.17 (4 H, m, aromatic), 7.45 (2 H, m, aromatic), 7.8 (1 H, s, Ar-CH), 11 (2 H, NH, s); LC/Q-TOF *m/z* 518.045 Anal. Calcd. for $C_{26}H_{20}BrN_3O_2S$: M + : 517.045403, M: 517.04596, [M + H] + : 518.053228; Found: *m/z*: M + : 517.04541, M: 517.04596, [M + H] + : 518.05324.

2.2.22. 2-{[2-(3H-indol-3-yl)ethyl]imino}-3-phenyl-5-[(2,5-dimethylphenyl)methylidene]-1,3-thiazolidin-4-one 19

1.5 mmol (0.5 g) of II, 4.5 mmol (0.6355 mL) of 2,5-dimethyl benzaldehyde and 3 mmol (0.30 mL) of piperidine were reacted in 2.5 mL of ethanol with as described in the general procedure III and recrystallized from 95% ethanol 78% yield as light yellow solid, mp:230–231 °C; FT-IR νmax (KBr, cm-1): 3352 (N-H), 3015–3057 (aromatic C═C-H), 2923 (aliphatic C-H), 1697 (C═O), 1596 (aromatic C═C), 1230 (C-N); 1H NMR δ ppm (400 MHz, DMSO-d6): δ/ppm 2.4 (3 H, CH_3, s), 2.6 (3 H, CH_3, s), 3.1 (2 H, t, CH_2 *J* = 7.1 Hz), 4.3 (2 H, CH_2 t, *J* = 6.9 Hz), 6.5 (8 H, m, aromatic), 6.91 (3 H, m, aromatic), 7.8 (1 H, s, Ar-CH), 7.9 (1 H, NH, s); LC/Q-TOF *m/z* 451.171 Anal. Calcd. for $C_{28}H_{25}N_3OS$: *m/z*: M + : 451.171284, M: 451.17183, [M + H] + : 452.179109; Found: *m/z*: M + : 451.17128, M: 451.17183, [M + H] + : 452.17911.

2.2.23. 2-{[2-(3H-indol-3-yl)ethyl]imino}-3-phenyl-5-[(3,5-dibromo-4-hydroxylphenyl)methylidene] −1,3-thiazolidin-4-one 20

1.5 mmol (0.5 g) of II, 4.5 mmol (1.3405 g) of 3,5-dibromo-4-hydroxy benzaldehyde and 3 mmol (0.30 mL) of piperidine were reacted in 2.5 mL of ethanol as described in the general procedure III and recrystallized from 95% ethanol with a 46% yield as light brown solid, mp: 211°C; FT-IR νmax (KBr, cm-1): 3473 (N-H), 3360 (OH), 3029 (aromatic C═C-H), 2954 (aliphatic C-H), 1701 (C═O), 1583–1610 (aromatic C═C), 1249 (C-N); 1 H NMR (400 MHz, DMSO-d6): δ/ppm = 3.1 (2 H, t, CH_2 *J* = 7.1 Hz), 4.1 (2 H, CH_2 t, *J* = 6.9 Hz), 6.8 (2 H, m, aromatic), 6.91 (1 H, m, aromatic), 7.17 (1 H, m, aromatic), 7.45 (2 H, m, aromatic), 7.62 (1 H, m, aromatic), 7.70 (5 H, m, aromatic), 7.8 (1 H, s, Ar-CH), 11 (1 H, NH, s); LC/Q-TOF *m/z* 594.956 Anal. Calcd. for $C_{26}H_{19}Br2N3O2S$: M + : 594.955908, M: 594.95647, [M + H] + : 595.963733; Found: *m/z*: M + : 594.95592, M: 594.95647, [M + H] + : 595.96375.

2.2.24. 2-{[2-(3H-indol-3-yl)ethyl]imino}-3-phenyl-5-[(3,4-dimethylphenyl)methylidene]-1,3-thiazolidin-4-one 21

1.5 mmol (0.5 g) of II, 4.5 mmol (0.6355 mL) of 3,4-dimethyl benzaldehyde and 3 mmol (0.30 mL) of piperidine were reacted in 2.5 mL of ethanol as described in the general procedure III and recrystallized from 95% ethanol with a 72% yield as yellow solid, mp:214°C; FT-IR νmax (KBr, cm-1): 3352 (N-H), 3015–3057 (aromatic C═C-H), 2923 (aliphatic C-H), 1697 (C═O), 1596 (aromatic C═C), 1230 (C-N); ^{1}H NMR (400 MHz, DMSO-d6): δ/ppm 3.1 (2 H, t, CH_2 *J* = 7.1 Hz), 4.1 (2 H, CH_2 t, *J* = 6.9 Hz), 6.8 (2 H, m, aromatic), 6.91 (1 H, m, aromatic), 7.17 (1 H, m, aromatic), 7.45 (2 H, m, aromatic), 7.62 (1 H, m, aromatic), 7.65 (5 H, m, aromatic), 7.8 (1 H, s, Ar-CH), 11 (1 H, NH, s). ^{13}C NMR δ ppm (400 MHz, DMSO-d6)δ/ppm = 19.83, 19.87, 23.25, 43.80, 111.00, 111.91, 118.63, 118.87, 120.31, 121.42, 121.48, 123.55, 125.23, 127.30, 127.72, 129.91, 130.79, 131.38, 131.77, 136.76, 137.71, 139.56, 148.35, 150.07, 166.23; LC/Q-TOF *m/z* 451.171 Anal. Calcd. for C28H24N3OS: M + : 451.171284, M: 451.17183, [M + H] + : 452.179109;Found: *m/z*: M + : 451.17128, M: 451.17183, [M + H] + : 452.17911.

2.2.25. 2-{[2-(3H-indol-3-yl)ethyl]imino}-3-phenyl-5-[(2,4,5-trimethoxy phenyl)methyl idene]-1,3-thiazolidin-4-one 22

1.5 mmol (0.5 g) of II, 4.5 mmol (0.8829 g) of 2,4,5-trimethoxy benzaldehyde and 3 mmol (0.30 mL) of piperidine were reacted in 2.5 mL of ethanol as described in the general procedure III and recrystallized from 95% ethanol with a 76% yield as yellow solid, mp:227 °C; FT-IR νmax (KBr, cm-1): 3456 (N-H), 3016–3059 (aromatic C═C-H), 2942 (aliphatic C-H), 1693(C═O), 1581 (aromatic C═C), 1271 (C-N); 1H-NMR (400 MHz, DMSO-d6):δ/ppm 3.1 = (2 H, t, CH_2 *J* = 7.1 Hz), 3.3 (3 H, s, OCH_3), 3.7 (3 H, s), 4.1 (2 H, CH_2 t, *J* = 6.9 Hz), 6.8 (2 H, m, aromatic), 6.91 (3 H, m, aromatic), 7.17 (1 H, m, aromatic), 7.45 (2 H, m, aromatic), 7.62 (3 H, m, aromatic), 7.8 (1 H, s, Ar-CH), 7.9 (1 H, NH, s); ^{13}C NMR (400 MHz, DMSO-d6) δ/ppm = 23.27, 43.66, 56.43, 56.88, 98.32, 110.93, 111.93, 112.74,113.33, 118.16, 118.63, 118.81, 121.43, 121.53, 123.53, 125.17, 125.55, 127.69, 129.80, 136.75, 143.10, 148.34, 150.32, 152.97, 154.51, 166.40; LC/Q-TOF *m/z* 513.172 Anal. Calcd. for $C_{29}H_{27}N_3O_4S$: M + : 513.171678, M: 513.17223, [M + H] + : 514.179503. Found: *m/z*: M + : 513.17168, M: 513.17223, [M + H] + : 514.1795.

2.2.26. {[2-(3H-indol-3-yl)ethyl]imino}-3-phenyl-5-[(3,5dichlorophenyl)methylidene]-1,3-thiazolidin-4-one 23

1.5 mmol (0.5 g) of II, 4.5 mmol (0.8119 mL) of 3,5-dichloro benzaldehyde and 3 mmol (0.30 mL) of piperidine were reacted in 2.5 mL of ethanol as described in the general procedure III and recrystallized from 95% ethanol with a 81% yield as yellow solid, mp:212.8°C; FT-IR νmax (KBr, cm-1): 3379 (N-H), 3011–3060 (aromatic C═C-H), 2984 (aliphatic C-H), 1704 (C═O), 1592–1607 (aromatic C═C), 1252 (C-N); ^{1}H NMR (400 MHz, DMSO-d6): δ/ppm = 3.1 (2 H, t, CH_2, *J* = 7.1 Hz), 4.1 (2 H, CH_2 t, *J* = 6.9 Hz), 6.8 (4 H, m, aromatic), 6.91 (2 H, m, aromatic), 7.17 (3 H, m, aromatic), 7.45 (2 H, m, aromatic), 7.62 (2 H, m, aromatic), 7.8 (1 H, s, Ar-CH), 11 (1 H, NH, s). ^{13}C NMR (400 MHz, DMSO-d6)δ/ppm = 23.19, 44.10, 110.78, 111.95, 118.54, 118.84, 121.35, 121.45, 123.62, 125.16, 125.52, 127.59, 127.66, 128.19, 129.45, 129.99, 135.24, 136.74, 137.40, 148.02, 149.08, 165.68; LC/Q-TOF *m/z* 491.062 Anal. Calcd. for $C_{26}H_{19}C_{l2}N_3OS$: M + : 491.062039, M: 491.06259, [M + H] + : 492.069864 Found: *m/z*: M + : 491.06204, M: 491.06259, [M + H] + : 492.06986.

2.2.27. 2-{[2-(3H-indol-3-yl)ethyl]imino}-3-phenyl-5-[(2,5-dichlorophenyl)methylidene]-1,3-thiazolidin-4-one 24

1.5 mmol (0.5 g) of II 4.5 mmol (0.8119 mL) of 2,5-dichloro benzaldehyde and 3 mmol (0.30 mL) of piperidine were reacted in 2.5 mL of ethanol were described in the general procedure III and purified by column chromatography with a 72% yield as yellow solid, mp:237 °C; FT-IR νmax (KBr, cm-1): 3379 (N-H), 3011–3060 (aromatic C═C-H), 2984 (aliphatic C-H), 1704 (C═O), 1592–1607 (aromatic C═C), 1252 (C-N). 1H-NMR (400 MHz, DMSO-d6): δ/ppm = 3.1 (2 H, t, CH_2, J = 7.1 Hz), 4.1 (2 H, CH_2 t, J = 6.9 Hz), 6.8 (2 H, m, aromatic), 6.91 (1 H, m, aromatic), 7.17 (1 H, m, aromatic), 7.45 (2 H, m, aromatic), 7.62 (4 H, m, aromatic), 7.7 (2 H, m, aromatic), 7.8 (1 H, s, Ar-CH), 11 (1 H, NH, s). ^{13}C NMR (400 MHz, DMSO) δ/ppm = 23.20, 44.14, 110.83, 111.93, 118.56, 118.90, 121.32, 121.51, 123.66, 124.56, 125.55, 127.22, 127.67, 128.37, 129.97, 131.45, 132.34, 132.75, 133.07, 133.77, 136.74, 148.01, 149.11, 165.46; LC/Q-TOF *m/z* 491.062 Anal. Calcd. for $C_{26}H_{19}C_{l2}N_3OS$: M + : 491.062039, M: 491.06259, [M + H] + : 492.069864; Found: *m/z*: M + : 491.06204, M: 491.06259, [M + H] + : 492.06986

2.3. Biology

2.3.1. Cell cultures

The human MCF7, A549 and PC3 cancer cell lines and non-cancerous human HUVEC cell line were grown in DMEM medium which was supplemented with 10% (v/v) Heat-inactivated fetal bovine serum (FBS), 2 mM L-glutamine and 50 unit/mL penicillin-streptomycin. Another human non-cancerous cell line MCF12A was grown in DMEM: F12 medium containing 5% (v/v) horse serum, 1 μg/mL insulin, 500 nM EGF and 50 unit/mL penicillin-streptomycin.

2.3.2. Cell viability assay

Cells were acutely treated with the compounds for which the dose response studies and viability analysis were tested. For viability analysis, a solution of 3-(4,5-dimethylthiazol-2-yl)-2,5-diphenyl tetrazoliumbromide (MTT), a yellow, water-soluble compound, was applied to the cells. When MTT is applied to living cells, it transforms into a blue-violet, water-insoluble reduced form, formazan. Determination of viable cell number was calculated by determining the color intensity obtained after dissolving formazan in alcohol by photometric measurements 2. To investigate the effect of the compounds on cancer cell proliferation, cells were seeded at a density of 3500/well in 96-well plate a day before treatment with the compounds. Subsequently, each compound was administered at 6 different concentrations (1,25–2,5–5–10–20–40 μM). After 72 h of incubation, formazan formation was determined for each concentration by applying MTT solution to the cells for 4 h and then solubilizing them in isopropanol. Effects of the compounds on cells' viability profiles were colorimetrically determined using Ascent Multiscan spectrophotometer at 570 nm. Tamoxifen, doxorubicin and 5-fluorouracil (5-FU) were used as reference drugs to compare the cytotoxic activity on cells. The percentage of viability by following formula: (CompoundAbs-BlankAbs) *100/(ControlAbs-BlankAbs), where the untreated cells were considered to demonstrate 100% viability.

Cytotoxic measurement parameter IC_{50} (inhibitory concentration by 50%), was calculated using curve fitting method on Excel and R_2 values were considered. Each compound was studied with 5 replicates. To determine the Selectivity Index (SI), each compound was applied on cancerous and non-cancerous cell lines to determine the selectivity of each compound against cancer cell targeted compound cytotoxicity. Accordingly, IC_{50} value of non-cancerous cell line was divided to IC_{50} value of cancer cell line and SI ≥ 1 depicted the selective action of the compound 3.

2.3.3. Tubulin polymerization assay

Tubulin polymerization followed by turbidity was performed using a microtubule polymerization assay kit (Cytoskeleton, BK011P) following the manufacturer's protocol. Briefly, porcine tubulin (3.6 mg/mL) in polymerization assay buffer (80 mM Pipes, pH 6.9, 2 mM MgCl2, 0.5 mM EGTA, 1 mM GTP, 10% glycerol) was added to pre-warmed 96-well microtiter plates at 37°C containing compound at IC50 concentrations in DMSO (final concentration 2%). After mixing, the rate of polymerization at 37°C was followed by absorption at 340 nm for 1 h at 2 min intervals using a Varioskan LUX Multimode Reader (Thermo Scientific). For this assay, vinblastine (3 μM) and paclitaxel (3 μM) were used as reference inhibitor, as the manufacturer suggested.

2.3.4. Tubulin polymerization imaging

MCF7 cells were seeded to 6-well plates containing cover slips with the initial cell number of 250 × 10^3/well. Next day cells were treated with/without compound for 24 h. After, media was removed and samples were washed three times with 1X PBS. Cell fixation was performed by addition %4 PFA for 20 min at room temperature. Then, cells were washed and permeabilized by 0.1% Triton X100 in PBS for 20 min at room temperature. After permeabilization, cells were blocked with 1% BSA for 30 min at room temperature. Blocking was followed by Tubulin labelling using primer anti-Tubulin (Protein-Tech, 66031–1-Ig) antibody (1:250) overnight at cold room. Alexa Fluor 488 anti-mouse secondary antibody (Abcam, ab150113) was applied to samples (1:200) for 45 min at 37 ℃. Nuclear staining was done by DAPI (Elabscience, E-CK-A163) for 10 min at room temperature. After washing steps, cells were mounted by Fluoromount-G (Invitrogen, 00495802) and cell imaging was performed using Zeiss Axio Fluorescence Microscope.

2.3.5. Wound healing assay

MCF7 cells were seeded in 6-well plates with the initial cell number of 5 × 10^5/well, and plates were incubated overnight to achieve monolayer cells. Then, the confluence of the cells was checked, and the scratches were made to each well using p200 pipette tips. After creating a scratch in each well, media were removed, and cells were washed with PBS until no floating cell were visible in the scratch area. Culture medium containing compound 15 was added with IC_{50} value, determined. Control cells were kept in

growing medium. Microscopic images of the scratches were taken and recorded at the same time each day for up to 96 h. Evaluation of the results were done by using Image J program by calculating the coverage area of the scratched region.

2.3.6. Cell cycle analysis

MCF7 cells were seeded in 6-well plates at a density of 5×10^5/well. After 24 h, cells were subjected to 4 h serum depleted media prior to the treatment of 3 μM of vinblastine and compound 15 with the respective IC_{50} concentration. Following the incubation period, cells were collected, fixed by 4% ethanol solution and cell cycle protocol was conducted by incubating samples in a mixture of 0.1% (v/v) triton X-100, 0.5 mg/mL RNaseA and 5 μg/mL PI solution. 20,000 events were analyzed by Guava easyCyte Flow Cytometer (Merck Millipore, Germany).

2.3.7. Annexin V/propidium iodide staining

To evaluate the apoptosis; 5×10^5 cells were seeded to cell culture dishes in triplicate and incubated overnight to allow attachment. Cells were then treated with the compound 15 at its' respective IC_{50} values, determined, for 24 h, after which the cells were collected by centrifuging cells at 300 g for 5 min. The pellet was suspended in 1 mL of Annexin V Binding Buffer (Abcam, #ab14084), and cells were labelled with Annexin V-FITC (1 μL, BioVision #1001) and PI (1 μL of 250 μg/mL in DPBS, Thermo Fisher Scientific, #P3566) by incubating at 4°C under dark conditions for 15 min. At the end of incubation, the tubes were analyzed with Beckman Coulter DxFLEX flow cytometry system. CytExpert for DxFLEX software was used for analysis. 2.5×10^4 events were analyzed for each tube. Each treatment group was compared with the control (untreated) group of the relevant cell line in terms of early apoptotic/apoptotic and necrotic cell populations.

2.4. Molecular modeling studies

Target protein, tubulin dimer composed of tubulin alpha and beta chain was retrieved from protein data bank PDB ID: 8V2I. This structure was further modified via first two/three probably damaging mutations retrieved from most frequent somatic mutations list in TCGA to represent a more realistic structure of tubulin in the setting of cancer. Introduced mutations on tubulin alpha 1b (Gene TUBA1B) were HIS197GLN, PRO248LEU and those for tubulin beta chain (Gene TUBB) were GLU194GLN, TYR398HIS and VAL439ASP. The structure was repaired for missing residues and were corrected for histidine protonation states via PDB2PQR program 5. This structure after modification was solvated and ionized using CHARMM-GUI and simulated for 100 ns using NAMD program 6 to get the root mean square displacement-based pose closest to the average structure. Average structure was further utilized in docking studies 7,8. The structure of positive control vinblastine and compounds (Compound 1–24) were designed via chemsketch program in mol format, and these structures were converted to pdb format via Avogadro program. The docking studies were carried out using Auto dock Vina 9. At the final step, selected docked complexes were further analyzed via PLIP program for weak interaction maps 10.

3. Results and discussion

3.1. Chemistry

A set of twenty four 5-(substituted) benzylidene-2-{[2-(3H-indol-3-yl)ethyl]imino}-3-phenyl-1,3-thiazolidin-4-one]) were synthesized through 3 steps as outline in (Scheme 1). Tryptamine and phenyl isothiocyanate combined in toluene at room temperature to yield of thiourea product **I**. Then, was reacted chloroacetyl chloride to produce 2-{[2-(3H-indol-3-yl) ethyl]imino}-3-phenyl-1,3-thiazolidin-4-one **II** in high yield. The final step was achieved, to the reacting II in the present of piperidine as base and the corresponding aromatic aldehyde to reach the final form of product **III** in yields ranging between 20% and 81%.

The molecular structure of compounds was verified by using FT-IR, ^{1}H NMR, ^{13}C NMR and HRMS (LC-MS/Q-TOF) spectroscopy techniques. In ^{1}H NMR spectra of the compounds aliphatic CH_2's showed up around at 2.30–4.33 ppm as triplets and the aromatic hydrogen atoms were around 6.93–8.31 ppm. The hydrogen atom of the NH in indole appeared at 6.23–10.64 ppm regarding the structure. Lastly, according to the substituent on the phenyl ring, different peaks were observed according to the functional group moiety.

Following evidences supported that both double bonds were in Z configuration. The configurations of exocyclic C═C and C═N bonds of synthetized compounds (1 − 24), on 2 and 5 positions of thiazolidone ring were elucidated using ^{1}H NMR, and geometry optimization using with density functional method DFT (TZVP). In ^{1}H NMR, the H atoms of methine proton on the C═C bonds of the thiazolidone ring gave a peak not over the 7.6 ppm which indicated Z isomer. Z configuration of exocyclic C═C bonds methine proton would be under deshielding effect of the of the carbonyl group thiazolidone ring at 4 position.[24,26] DFT results also showed that the lowest-energy conformers correspond to the Z isomers, rather than E conformation as reported by Wang et al. in 2011.[27] Details were provided in supporting information.

In the ^{13}C NMR spectra of aliphatic two CH_2 groups of the compounds, appeared at around 35.79–42.75 ppm. Aromatic carbon atoms of the compounds gave the peak at 114.91–143.26 ppm. The carbonyl carbons of the ketone in the thiazoldine-4-one ring structure appeared at 186.72–189.33 ppm. LC-MS/Q-TOF. Results were given as exact mass. Details given in supporting information.

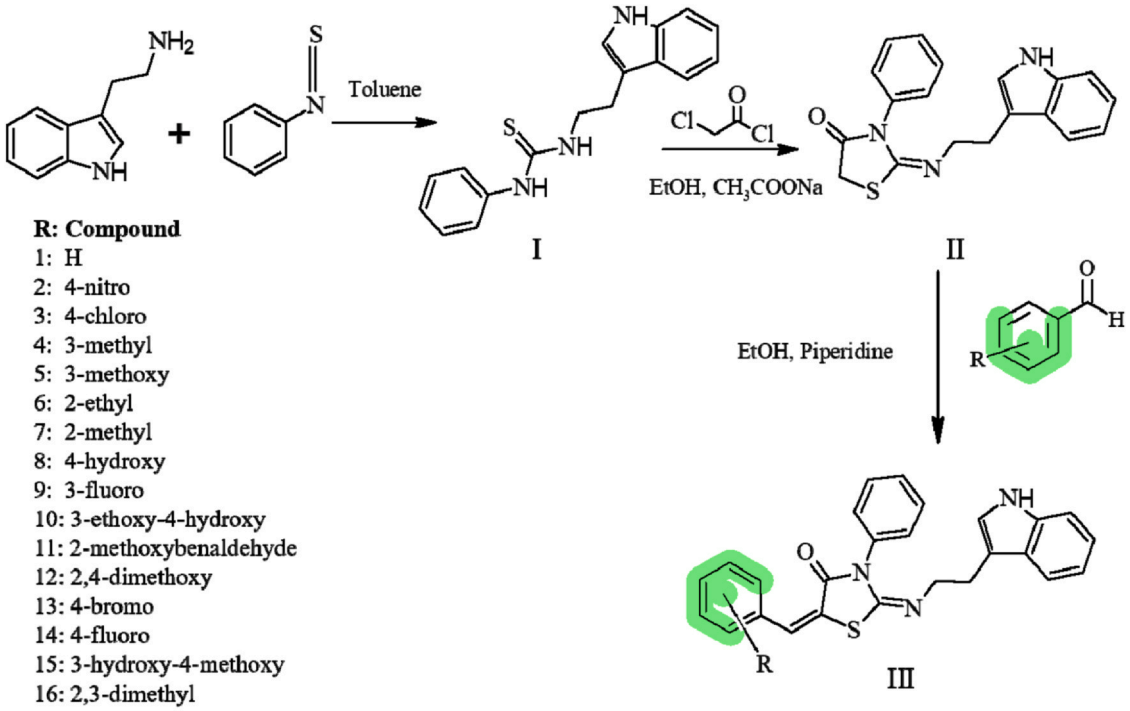

Scheme 1. General synthesis of Indole-Thiazolidin-4-one Hybrid Molecules.

3.2. Biology

3.2.1. In vitro antiproliferative activity

Antiproliferative activity of the all-synthesized compounds (1 − 24) were performed on breast cancer cell line (MCF7), non-tumorigenic mammary epithelial cells (MCF12A), Human Umbilical Vein Endothelial Cell (HUVEC), adenocarcinoma human alveolar basal epithelial cells (A549) and human prostate cancer cell line (PC3) using MTT assay. Table 1 showed the result of the thiazolidin-4-one-indole hybrid derivatives on the cell line with IC_{50} (μM) values. The tested compounds showed excellent to moderate anti-proliferative activity according to their substituted moiety.

MCF7, MCF12A, HUVEC, A549 and PC3 were used to evaluate the target compounds for cytotoxicity by MTT method using Tamoxifen, Doxorubicin, 5-fluorouracil, and Vinblastine as the reference compounds. The results were summarized in Table 1. As the table showed, compounds, 8, 10, 15, 21 and 23 were determined as the most active on these cell lines based on their SI values. SI values were determined > 1 (ranging between 1.03704 and 3.70588), indicating that compounds were acting selectively. It might be deduced that the presence of 4-hydroxy substituted on benzylidene moiety (compound 8) was cytotoxic on only MCF7 while 3-ethoxy-4-hydroxy substitution possessing (compound 10) exerted cytotoxic activity against all cancerous cell lines; MCF7, A549 and PC3, selectively. Compound 15 with 3-hydroxy-4-methoxy, compound 21 with 3,4-dimethyl and compound 23 with 3,5-dicholoro substitutions on benzylidene moieties demonstrated cytotoxic activity on MCF7 and A549 cell lines. When cell viability profiles were tested, all compounds chosen showed their activities in dose dependent manner (Fig. 3).

3.2.2. Tubulin polymerization studies

The selected compounds were subjected to tubulin protein polymerization assay to investigate their ability to inhibit tubulin polymerization. The effects of the derivatives selected, were compared to paclitaxel and vinblastine administered as reference controls. Their evaluation of tubulin polymerization inhibition revealed compelling behavior of those selected compounds (Fig. 4 & Figure S89).

Table 1
Cytotoxic effects of The Thiazolidin-4-One-Indole Hybrid Derivatives against MCF7, A549 and PC3 Cancer Cell Lines.

	MCF7			MCF12A		HUVEC		A549			PC3		
Compound	**IC_{50} (μM)**	**R^2**	**SI > 1.0**	**IC_{50} (μM)**	**R^2**	**IC_{50} (μM)**	**R^2**	**IC_{50} (μM)**	**R^2**	**SI > 1.0**	**IC_{50} (μM)**	**R^2**	**SI > 1.0**
1	25	0,95	1,3	32	0,90	14	0,85	23	0,94	0,61	25	0,91	0,56
2	48	0,94	0,5	26	0,97	17	0,85	10	0,95	1,70	73	0,90	0,23
3	17	0,94	1,1	19	0,91	29	0,91	29	0,90	1,00	44	0,90	0,66
4	20	0,94	1,4	28	0,92	19	0,86	43	0,90	0,44	49	0,91	0,39
5	17	0,92	1,1	19	0,92	15	0,88	40	0,92	0,38	35	0,90	0,43
6	20	0,93	0,8	15	0,95	23	0,97	36	0,94	0,64	33	0,98	0,70
7	29	0,94	1,0	28	0,97	32	0,86	23	0,91	1,39	30	0,93	1,07
8	**13,5**	0,95	**1,0**	14	0,90	16	0,96	23	0,97	0,70	17	0,99	0,94
9	26	0,96	0,7	19	0,93	28	0,98	49	0,83	0,57	12	0,92	2,33
10	**13**	0,96	**2,2**	29	0,95	23	0,95	**21**	0,90	**1,10**	**8**	0,96	**2,88**
11	28,5	0,96	0,5	14	0,98	43	0,93	43	0,96	1,00	44	0,90	0,98
12	47	0,94	0,1	4	0,93	21	0,86	104	0,85	0,20	107	0,91	0,20
13	22	0,94	0,5	11	0,90	19	0,90	19	0,90	1,00	28	0,90	0,68
14	55	0,91	0,7	38	0,95	152	0,91	110	0,91	1,38	101	0,93	1,50
15	**17**	0,92	**3,7**	63	0,91	18	0,90	**17**	0,90	**1,06**	22	0,93	0,82
16	16	0,96	1,1	17	0,95	34	0,93	37	0,91	0,92	31	0,90	1,10
17	26	0,99	0,6	16	0,95	54	0,92	23	0,96	2,35	53	0,90	1,02
18	21	0,96	0,7	15	0,92	20	0,99	15	0,91	1,33	23	0,92	0,87
19	46	0,96	0,3	12	0,90	22	0,94	52	0,92	0,42	33	0,99	0,67
20	29	0,97	0,4	13	0,93	18	0,91	76	0,92	0,24	25	0,94	0,72
21	**22**	0,95	**1,1**	25	0,99	21	0,96	**12**	0,91	**1,75**	27	0,91	0,78
22	7	0,90	1,3	9	0,96	8	0,90	16	0,92	0,50	28	0,93	0,29
23	**19**	0,90	**1,4**	26	0,98	22	0,96	**14**	0,91	**1,57**	28	0,95	0,79
24	12	0,90	1,8	21	0,96	18	0,90	29	0,90	0,62	27	0,91	0,67
Tamoxifen	13	0,91	1,1	14	0,91	21	0,91	25	0,92	0,84	22	0,95	0,95
Doxorubicin	0,5	0,99	3,4	1,7	0,99	0,92	0,96	0,84	0,83	1,10	15	0,92	0,06
5-FU	5	0,90	0,8	4	0,90	6	0,93	5	0,95	1,20	6	0,97	1,00
Vinblastine	0,8	0,96	0,4	0,3	0,90	0,005	0,95	0,5	0,8	0,01	ND	-	-

Positive control. IC_{50} (μM) and SI values for each cancer cell types were calculated. **Compounds with IC_{50} values, selected for mechanistic studies are marked in bold.**

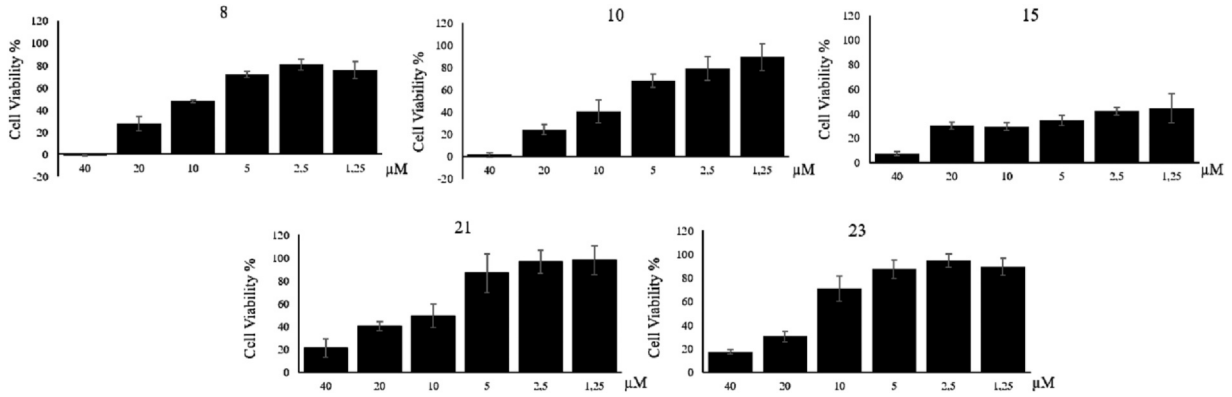

Fig. 3. MCF7 cell viability upon the treatment of the compounds, 8, 10, 15, 21 and 23 respectively. Cell were subjected to the compounds indicated for 72 h. MTT assay was applied to check the cell viability. Each compound was tested in 5 replicates at least 2 times. Data mean ± SD.

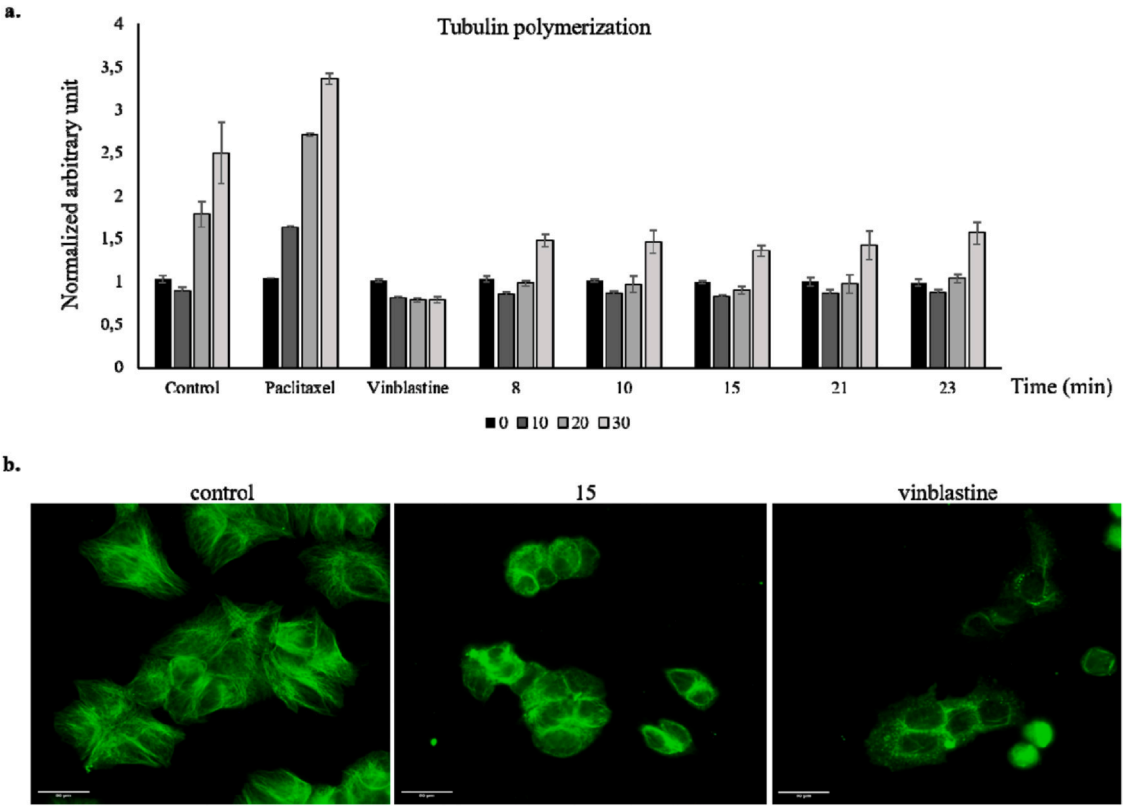

Fig. 4. a. Tubulin Polymerization in the Presence of Compounds 8, 10, 15, 21 and 23. Tubulin protein assay was performed testing the compounds indicated. Polymerization was measured fluorometrically. Samples gained data was normalized to zero moment control. 6 replicates were tested. Data mean ± SD. b. Fluorescent microscopy images of MCF7 cells treated with compound 15 and vinblastine as indicated. Scale bar 50 μM.

The initial 20 min of the experiment demonstrated a potent inhibitory effect in similar to vinblastine, showing their rapid activity by inhibiting of tubulin polymerization. However, starting from 30th minute on, we observed a gradual increase in tubulin polymerization, likely, due to a potential dissociation of these selected compounds. Notably, after 60 min, vinblastine maintained its inhibitory activity, while the activity of the

synthesized compounds' inhibitory effect notably decreased, however they remained superior to the controlled group without tubulin polymerization inhibitors (Figure S89). In contrast, paclitaxel, known for its tubulin polymerization enhancement, exhibited a distinct pattern. Unlike the synthesized compounds, paclitaxel demonstrated an increase in polymerization state. Results suggested that compounds exhibited a mild inhibition on tubulin polymerization in the same fashion with Vinblastine mediated tubulin polymerization. Their evaluation of tubulin polymerization inhibition revealed compelling behavior of those selected compounds were given in (Fig. 4a).

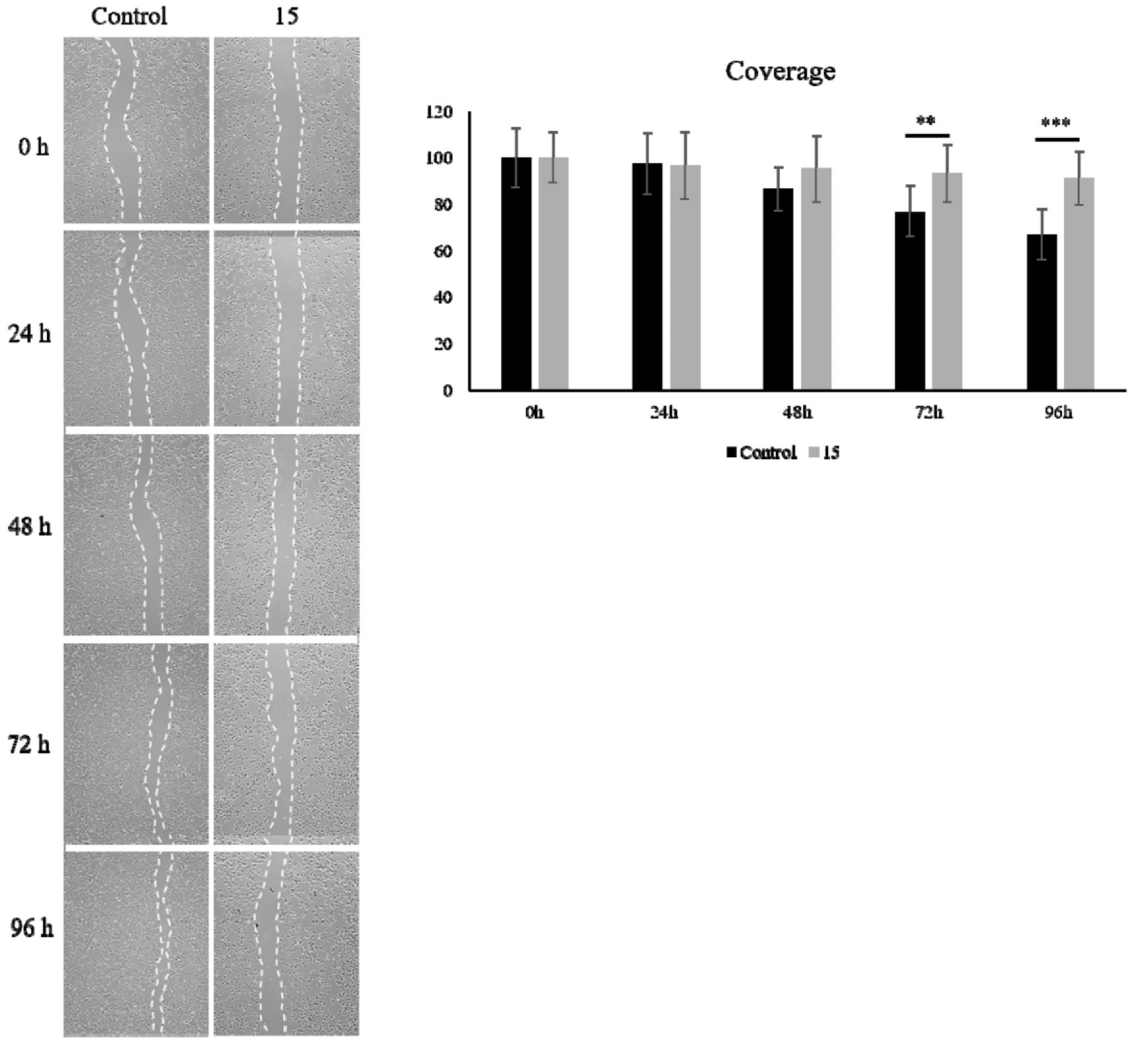

Fig. 5. Scratch assay to assess the effect of compound 15 on cell migration. Images of the scratch area of MCF7 cell population were taken at the indicated time points (0,24,48,72 and 96 h). Coverage of scratch area was calculated using ImageJ. Experiments were performed 3 times. Data mean ± SD (***p ≤ 0.001, p** ≤ 0.01).

Amongst direct targeting the polymerization dynamics of Tubulin network, depolymerization mode of action can affect cell morphology as well as mitotic spindle occurrence.[28] In our study, compounds tested were also applied to MCF7 cells to monitor the alterations of tubulin polymerization. Of the compounds, compound 15 treatment showed inhibition on tubulin polymerization. Cells were more rounded up and tubulin network was defragmented, partially (Fig. 4b). Complete inhibition of tubulin polymerization was detected upon vinblastine treatment. The effect of the compound 15 was rather slight compared to vinblastine, as the *ex vivo* assay results demonstrated the short-term strong effect on tubulin polymerization (Fig. 4a).

3.2.3. Migration and cell death studies

In order to investigate the cell-based effects of compound 15, monolayer formed MCF7 cells were grown and scratch was generated using pipet tip. Scratch images were taken using Invitrogen EVOS xl core imaging system every 24 h (Fig. 5). Results demonstrated that compound 15 administered with respective IC_{50} concentration, MCF7 cells could cover the scratched area significantly less than untreated control cells. After 96 h of scratch formation the coverage of the region was 33% on untreated cells whereas this coverage was observed only 9% on compound 15 treated cells (Fig. 5). The effect of compound 15 application suggested an inhibition on cell movement in MCF7 cells.

Cell death mechanism studies revealed that compound 15 decreased viability in MCF7 cell line after 24 h. Compound 15 treatment demonstrated a decreased early apoptotic population in MCF7 cells which was similar to vinblastine treated cell population. Moreover, administration of compound 15 significantly increased late apoptosis which was in line with vinblastine treatment. Necrotic cell population was detected upon compound 15 treatment; however, its effect was less pronounced when compared to vinblastine administered one (Fig. 6).

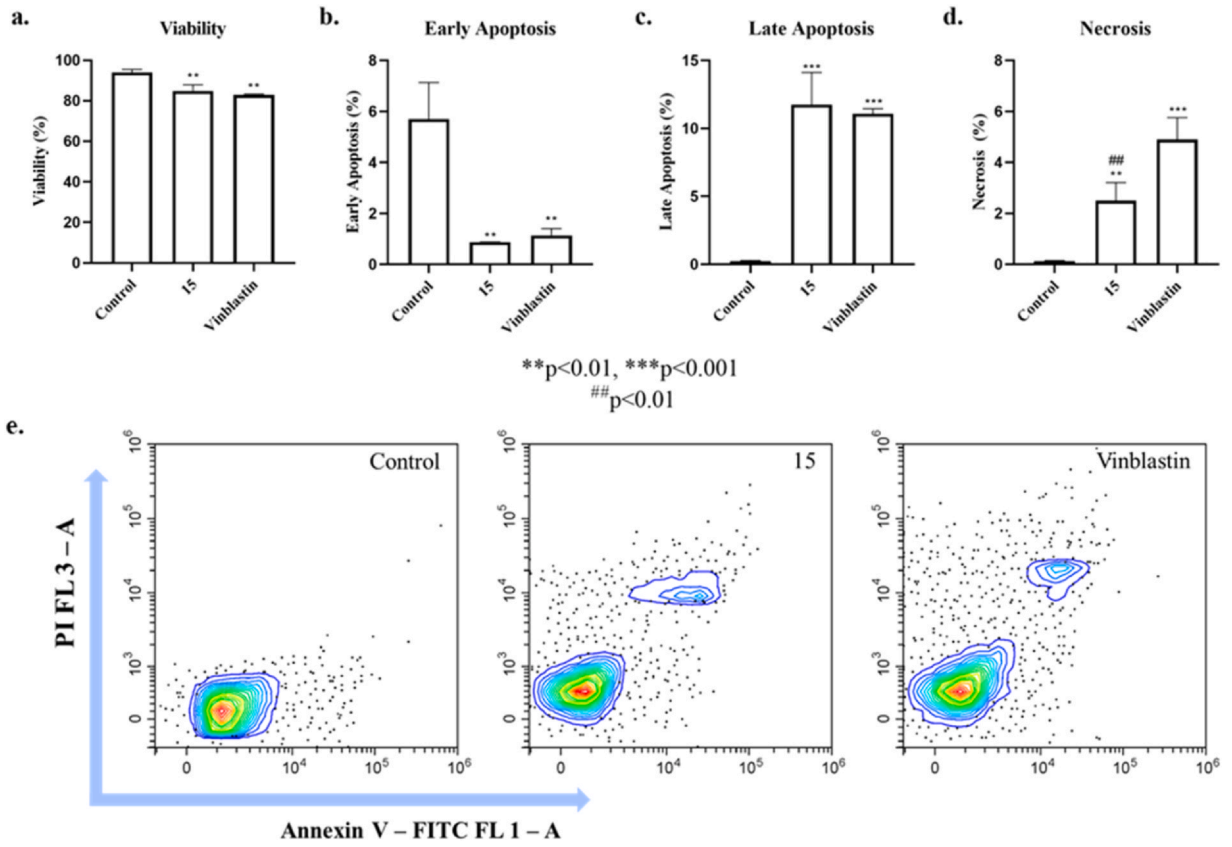

Fig. 6. Cell death mechanisms profiles of the compound 15. MCF7 cells were treated with 15 and with the reference drug vinblastine. Cell viability a. early b. and late c. apoptosis, and necrosis d. were investigated. Representative flow cytometry contour plots were shown in (e.). Asterisk and hash symbols indicate differences between the untreated control and compound 15; and differences between vinblastine and the compound 15, respectively. (***p ≤ 0.001, ** p ≤ 0.01; ### p ≤ 0.001, p## ≤0.01). Data mean ± SD.

To find out the effect of compound 15 on cell cycle arrest, MCF7 cells were treated with the 3 μM vinblastine and compound 15 with respective IC_{50} concentration for 24 h. The average G0/G1 cell population for control, 3 μM vinblastine treated and compound 15 treated MCF7 cells were found as 49.81%, 54.44% and 58.18% respectively. The average percentage of S phase for untreated MCF7 cells was 19.89%, while vinblastine and compound 15 treated cell percentages were found as 6.77% and 4.71% respectively. The population of cells in G2/M phase was 26.11% and 19.46% after the treatment with vinblastine and compound 15. For the control group, the frequency of G2/M cell cycle phase was found as 19.28% (Fig. 7).

3.3. Molecular docking and interaction studies

In order to get a better understanding of how newly designed ligands are preferring to bind tubulin, a molecular docking study was implemented. The target tubulin dimer is retrieved from protein databank (PDB ID:8V2I). This dimeric tubulin structure was further subjected to structural repairing for missing residues, and to mutations in order to mimic cancerous phenotype and to assignments of histidine protonation states. For the docking step, vinblastine, was used as the positive control ligand.[29] The binding site of the vinblastine resides between the dimerization interface as shown in Fig. 8.[30] This site was used as a binding site for all newly synthesized small ligands as well as the positive control vinblastine. The results of the Autodock Vina[31] based docking was summarized in Table 2. It was apparent that docking program utilized could distinguish that all of the ligands are better binders to the tubulin dimer interface as compared with the positive control vinblastine (Table 2).

All the compound listed were docked to the tubulin dimer composed of tubulin alpha and beta chain, which was retrieved from protein data bank PDB ID: 8V2I using Autodock Vina program. Negative affinity value corresponds to a more possible binding model and these molecules would be likely to bind.

A next, tubulin dimer docked to compound 8, 10, 15, 21 and 23 were compared with their counterpart bound to vinblastine using PLIP program (Table 3).[32] Within the tested compounds, all have presented some degree of similarity within their molecular interaction map compared with vinblastine (Table 3). More specifically all of the complexes had either very close allocated residues or same residues for hydrophobic contacts, hydrogen bonding and salt bridges in between target and ligand, compared with vinblastine

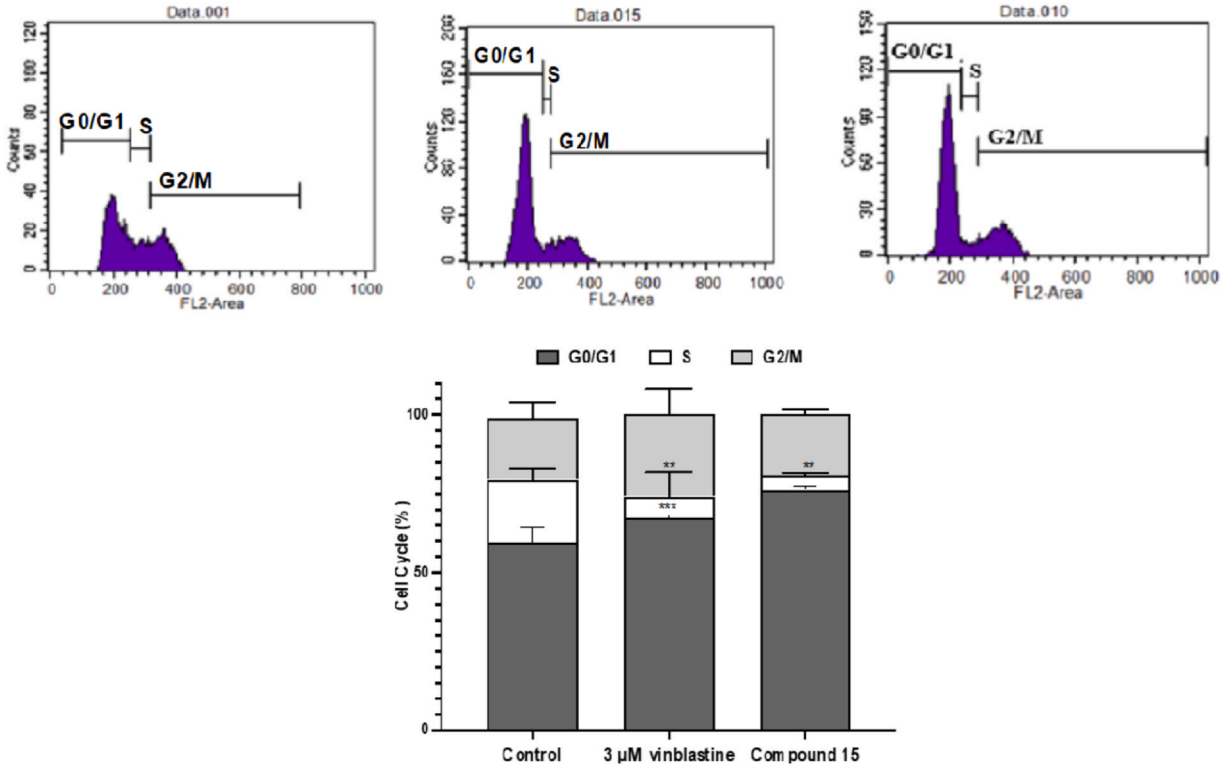

Fig. 7. Cell cycle profiles of MCF7 cells, examined by flow cytometry. The plots of control MCF7 cells, 3 µM vinblastine treated MCF7 cells, Compound 15 treated MCF7 cells were indicated, respectively. Overall cell cycle profiles after treatment with the compound 15 and vinblastine. (***p ≤ 0.001, p** ≤0.01). Data mean ± SD.

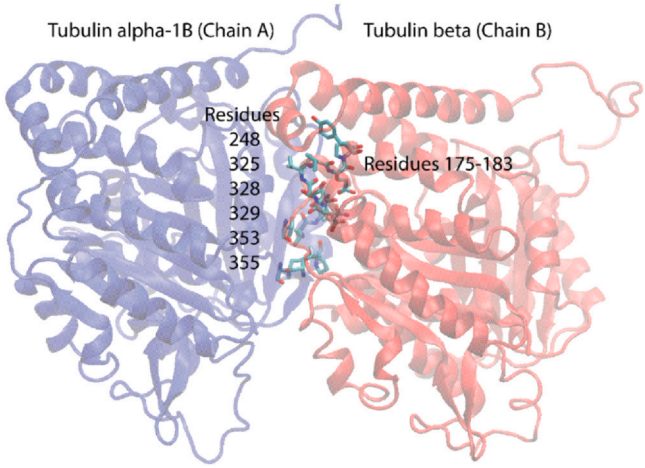

Fig. 8. The tubulin dimer structure and residues used for docking studies. The structure was retrieved from protein data bank (PDB ID:8V2I). Cancer related mutations mentioned in materials & methods section were introduced into the structure to get a more realistic tubulin dimer associated with cancer. Residues shown in the figure matches to the region where vinblastine is binding and these residues were used to generate the probable binding site during the docking procedure of newly designed small molecule ligands.

containing tubulin dimer complex (Table 3). In conclusion, molecular docking and interaction studies pointed out compounds 8, 10, 15, 21 and 23 as the most plausible candidate for inhibiting tubulin dimerization as supported ex vivo studies.

Tubulin dimer docked structures of each compound were analysed via PLIP program to retrieve possible weak interaction maps in between protein and compound. Dist.: Distance.

Similar approach had been reported by Khan *et al.* that molecular docking results of thiazole-linked thiazolidinone substituents especially a para-hydroxy (-OH) group on the phenyl ring exhibit strong binding through a combination of hydrogen bonds, hydrophobic interactions, and electrostatic forces.[21]

Table 2
Autodock Vina based affinities of the compounds tested.

Compound No	Autodock Vina determined affinity (kcal/mol)
Positive Control (Vinblastine)	**-0.10**
Compound 1	-8.00
Compound 2	-8.30
Compound 3	-8.10
Compound 4	-8.00
Compound 5	-8.00
Compound 6	-8.20
Compound 7	-8.30
Compound 8	**-8.40**
Compound 9	-8.20
Compound 10	**-8.00**
Compound 11	-8.20
Compound 12	-8.30
Compound 13	-8.00
Compound 14	-8.10
Compound 15	**-8.10**
Compound 16	-9.20
Compound 17	-8.00
Compound 18	-9.10
Compound 19	-8.50
Compound 20	-9.30
Compound 21	**-8.10**
Compound 22	-8.20
Compound 23	**-8.30**
Compound 24	-8.10

Table 3
Molecular interaction analyses for Positive Control (Vinblastine) and the Compounds 8, 10, 15, 21 and 23.

Ligand name	Important Residues identified by PLIP
Vinblastine	Hydrophobic interactions (Chain A): Leu 248 (Dist.: 2.94). Hydrophobic Interactions (Chain B): Gln 11 (Dist.: 3.25), Leu 68 (Dist.: 3.49), Val 169 (Dist.: 3.13 and 3.94), Val 175 (Dist.: 3.58), Tyr 222 (Dist.: 3.93). Hydrogen bonds (Chain A): Asn 249 (Dist: 2.83). Hydrogen bonds (Chain B): Gln 11 (Dist: 2.84), Asn 99 (Dist: 3.45), Gly 144 (Dist.: 3.25), Asp 177 (Dist.: 3.10 and 3.18), Asn 204 (Dist: 2.81). Salt bridges (Chain A): Glu 254 (Dist: 3.80). Salt bridges (Chain B): Asp 177 (Dist: 4.83).
Compound 8	Hydrophobic Interactions (Chain B): Gln 11 (Dist.: 3.77) Hydrogen bonds (Chain B): Ser 138 (Dist: 2.28), Gly 144 (Dist.: 2.26). Salt bridges (Chain B): Asp 177 (Dist.: 3.99).
Compound 10	Hydrophobic Interactions (Chain B): Gln 11 (Dist.: 3.82), Leu 68 (Dist.: 3.62). Salt bridges (Chain B): Asp 67 (Dist: 4.92).
Compound 15	Hydrophobic Interactions (Chain B): Gln 11 (Dist.: 3.94), Leu 68 (Dist.: 3.71). Hydrogen bonds (Chain B): Ser 138 (Dist.: 3.38). Salt bridges (Chain B): Asp 67 (Dist.: 4.73).
Compound 21	Hydrophobic interactions (Chain A): Asp 251 (Dist.: 3.97), Glu 254 (Dist.: 3.86) Hydrophobic Interactions (Chain B): Gln 11 (Dist.: 3.53), Leu 68 (Dist.: 3.85), Thr 143 (Dist.: 3.63). Hydrogen bonds (Chain A): Lys 352 (Dist.: 3.12). Hydrogen bonds (Chain B): Gln 11 (Dist.: 3.23). Salt bridges (Chain A): Glu 254 (Dist.: 4.16). Salt bridges (Chain B): Asp 177 (Dist.: 5.15).
Compound 23	Hydrophobic Interactions (Chain B): Asp 177 (Dist.: 3.93). Hydrogen bonds (Chain B): Gly 144 (Dist.: 2.42). Salt bridges (Chain B): Asp 177 (Dist.: 5.25).

3.4. Calculation of ADME properties

In-silico studies were done by SwissADME module by Swiss Institute of Bioinformatics. ADME (absorption, distribution, metabolism, and excretion) parameters of tested compounds were calculated by SwissADME module theoretically.[33] Overall, compounds have acceptable potency to the receptors due to the ability to form hydrogen bonds. The (log Po/w) is found to be > 3 which indicates that they are more hydrophobic and have a higher affinity for non-polar environments like lipid membranes, show high absorption in the gastrointestinal tract and no passages to cross the blood brain barrier. In addition, the different hepatic enzymes that could lead into the metabolism of those compounds in Supplementary Table S5 and S6.

4. Conclusion

Twenty-four 5-(substituted) benzylidene-2-{[2-(3H-indol-3-yl)ethyl]imino}-3-phenyl-1,3-thiazolidin-4-one derivatives were synthesized through a three-step protocol. Structure elucidation was performed using analytical techniques including FT-IR, ^{1}H NMR, ^{13}C NMR, and LC-MS/Q-TOF. The synthesized compounds (1–24) demonstrated antiproliferative activity against MCF7, A549, and PC3 cell lines. In addition to IC_{50} values, selectivity indexes were calculated; compounds 8, 10, 15, 21, and 23 showed the highest cytotoxic activities against MCF7. When these compounds were applied to pure tubulin protein at their IC_{50} values to monitor polymerization, a vinblastine-like inhibitory effect was detected within the first 20 min. In silico molecular docking and weak interaction analyses indicated that all selected compounds were better binders than vinblastine on the tubulin dimer. ADME properties were also calculated using the SwissADME module indicated that compounds displayed highly hydrophobic characteristics. Of the selected compounds, Compound 15 inhibited cell migration, which aligned with its effect on tubulin polymerization. Furthermore, cells treated with Compound 15 displayed G0/G1 accumulation and apoptotic populations, suggesting that the inhibition of tubulin polymerization triggered cell death. In conclusion, Compound 15, possessing a 3-hydroxy-4-methoxy substitution on the benzylidene moiety, exhibited a structural pattern that was highly effective. This combination balanced strong hydrogen bonding, optimized steric fit, and favorable hydrophobic interactions, which collectively established Compound 15 as a potential hit molecule and encourages further studies to develop it as a potent tubulin polymerization inhibitor.

Lists of abbreviations

FT-IR, Fourier transform infrared spectroscopy; ^{1}H NMR, proton nuclear magnetic resonance; ^{13}C NMR, carbon-13 nuclear magnetic resonance; LC/MS, Liquid chromatography/mass spectrometry; LC/Q-TOF, Liquid chromatography/quadrupole-time of flight; HRMS, high-resolution mass spectrometry; PLIP, Protein–ligand interaction profiler; DFT (TZVP), Density functional theory (triple-zeta valence with polarization basis set); MTT, 3-(4,5-dimethylthiazol-2-yl)-2,5-diphenyltetrazolium bromide; IC_{50}, half maximal inhibitory concentration; SI, Selectivity index.

Supporting information

General procedures for chemistry, experimental procedures for the synthesis of compounds; structures and characterization data including FT-IR, ^{1}H NMR, ^{13}C NMR and HRMS (LC-MS/Q-TOF) spectroscopy data of all compounds, experimental details about biological assays, DFT calculations and configurations of the selected compound, supporting experimental figure, and ADME properties (PDF).

CRediT authorship contribution statement

Dilek Telci: Writing – review & editing. **Ipek Bedir:** Investigation. **Gülderen Yanıkkaya Demirel:** Writing – review & editing. **Başak Aru:** Investigation. **Ahmet Can Timuçin:** Writing – review & editing, Methodology. **Güneş Yıldırım Akdeniz:** Methodology, Investigation. **Hülya Akgün:** Writing – review & editing, Writing – original draft, Supervision, Conceptualization. **Burcin Gungor:** Writing – review & editing, Writing – original draft, Project administration, Methodology, Funding acquisition, Data curation, Conceptualization. **Naz Unal:** Methodology, Investigation. **Abdulrahman Abba:** Methodology, Investigation. **Zulal Sevgi Dede:** Investigation.

Ethics approval and consent to participate

Not applicable.

Funding

There is no funding to report.

Data availability statement

The datasets used and analysed during the current study are available from the corresponding author on reasonable request.

Declaration of Competing Interest

The authors declare the following financial interests/personal relationships which may be considered as potential competing interests: Burcin Gungor reports financial support was provided by Health Institutes of Turkey. If there are other authors, they declare that they have no known competing financial interests or personal relationships that could have appeared to influence the work reported in this paper.

Acknowledgement

The authors appreciate the financial support of Health Institutes of Türkiye (TUSEB) under the grant number 20148. We are thankful to Prof. Dr. Hakan Göker for the instrumental analysis. Special thanks to Dr. Suhaib Shekfeh for performing DFT calculations.

Appendix A. Supporting information

Supplementary data associated with this article can be found in the online version at doi:10.1016/j.lddd.2026.100367.

References

1. Jordan MA, Wilson L. Microtubules as a target for anticancer drugs. *Nat Rev Cancer.* 2004;4:253–265. https://doi.org/10.1038/NRC1317
2. Yang H, Ganguly A, Cabral F. Inhibition of cell migration and cell division correlates with distinct effects of microtubule inhibiting drugs. *J Biol Chem.* 2010;285:32242. https://doi.org/10.1074/JBC.M110.160820
3. Almagro L, Fernández-Pérez F, Pedreño MA. Indole alkaloids from Catharanthus roseus: bioproduction and their effect on human health. *Molecules.* 2015;20:2973–3000. https://doi.org/10.3390/MOLECULES20022973
4. Hill SA, Lonergan SJ, Denekamp J, Chaplin DJ. Vinca alkaloids: anti-vascular effects in a murine tumour. *Eur J Cancer.* 1993;29A:1320–1324. https://doi.org/10.1016/0959-8049(93)90082-Q
5. Liu L, O'kelly D, Schuetze R, et al. Non-invasive evaluation of acute effects of tubulin binding agents: a review of imaging vascular disruption in tumors. Page 2551 26 *Molecules 2021.* 2021;26:2551. https://doi.org/10.3390/MOLECULES26092551
6. Jia Y, Wen X, Gong Y, Wang X. Current scenario of indole derivatives with potential anti-drug-resistant cancer activity. *Eur J Med Chem.* 2020;200. https://doi.org/10.1016/J.EJMECH.2020.112359
7. Chadha N, Silakari O. Indoles as therapeutics of interest in medicinal chemistry: bird's eye view. *Eur J Med Chem.* 2017;134:159–184. https://doi.org/10.1016/J.EJMECH.2017.04.003
8. Kumari A, Singh RK. Medicinal chemistry of indole derivatives: current to future therapeutic prospectives. *Bioorg Chem.* 2019;89:103021. https://doi.org/10.1016/J.BIOORG.2019.103021
9. F.C. Brown, 4-Thiazolidinones, Chem Rev 61 (1961) 463–521. https://doi.org/10.1021/CR60213A002/ASSET/CR60213A002.FP.PNG_V03.
10. Gupta A, Singh R, Sonar PK, Saraf SK. Novel 4-thiazolidinone derivatives as anti-infective agents: synthesis, characterization, and antimicrobial evaluation. *Biochem Res Int.* 2016;2016:8086762. https://doi.org/10.1155/2016/8086762
11. Pitta E, Tsolaki E, Geronikaki A, et al. 4-thiazolidinone derivatives as potent antimicrobial agents: microwave-assisted synthesis, biological evaluation and docking studies. *Medchemcomm.* 2015;6:319–326. https://doi.org/10.1039/C4MD00399C
12. Samadhiya P, Sharma R, Srivastava SK, Srivastava SD. Synthesis and biological evaluation of 4-thiazolidinone derivatives as antitubercular and antimicrobial agents. *Arab J Chem.* 2014;7:657–665. https://doi.org/10.1016/J.ARABJC.2010.11.015
13. El-Adl K, Sakr H, Nasser M, Alswah M, Shoman FMA. 5-(4-Methoxybenzylidene)thiazolidine-2,4-dione-derived VEGFR-2 inhibitors: design, synthesis, molecular docking, and anticancer evaluations. *Arch Pharm (Weinh.* 2020;353. https://doi.org/10.1002/ARDP.202000079
14. El-Adl K, El-Helby AGA, Sakr H, Eissa IH, El-Hddad SSA, M.I.A. Shoman F. Design, synthesis, molecular docking and anticancer evaluations of 5-benzylidenethiazolidine-2,4-dione derivatives targeting VEGFR-2 enzyme. *Bioorg Chem.* 2020;102:104059. https://doi.org/10.1016/J.BIOORG.2020.104059
15. Al-Behery AS, Elberembally KM, Eldawy MA. Synthesis, docking, and biological evaluation of thiazolidinone derivatives against hepatitis C virus genotype 4a. *Med Chem Res.* 2021;30:1151–1165. https://doi.org/10.1007/S00044-021-02721-W
16. Chitre TS, Patil SM, Sujalegaonkar AG, Asgaonkar KD. Designing of thiazolidin-4-one pharmacophore using qsar studies for anti-hiv activity. *Indian J Pharm Educ Res.* 2021;55:581–589. https://doi.org/10.5530/IJPER.55.2.97
17. Omar YM, Abdel-Moty SG, Abdu-Allah HHM. Further insight into the dual COX-2 and 15-LOX anti-inflammatory activity of 1,3,4-thiadiazole-thiazolidinone hybrids: the contribution of the substituents at 5th positions is size dependent. *Bioorg Chem.* 2020;97:103657. https://doi.org/10.1016/J.BIOORG.2020.103657
18. Fettach S, Thari FZ, Hafidi Z, et al. Synthesis, α-glucosidase and α-amylase inhibitory activities, acute toxicity and molecular docking studies of thiazolidine-2,4-diones derivatives. *J Biomol Struct Dyn.* 2022;40:8340–8351. https://doi.org/10.1080/07391102.2021.1911854
19. Khan Y, Hussain R, Rehman W, et al. In-vitro and in-silico assessment of thiazole-thiazolidinone derivatives as selective inhibitors of urease and α-glucosidase. *Future Med Chem.* 2024;16:2627. https://doi.org/10.1080/17568919.2024.2432303
20. Khan Y, Khan S, Hussain R, Mukhtar A, Sarfraz H, Aminullah S. Medicinal approaches toward diabetes mellitus based on chloro-1H-indazole-derived triazolo-thiadiazole hybrid derivatives: design, synthesis, characterization, in vitro and in silico insights. *J Iran Chem Soc.* 2025;22:1209–1227. https://doi.org/10.1007/s13738-025-03216-w
21. Farghaly TA, Rehman W, Khan Y, Sarfraz H. Synthesis, biological screening and computational analysis of Thiazole linked Thiazolidinone Schiff bases as anti-Alzheimer's drug candidates. *Bioorg Chem.* 2025;164:108812. https://doi.org/10.1016/J.BIOORG.2025.108812
22. Beharry Z, Zemskova M, Mahajan S, et al. Novel benzylidene-thiazolidine-2,4-diones inhibit Pim protein kinase activity and induce cell cycle arrest in leukemia and prostate cancer cells. *Mol Cancer Ther.* 2009;8:1473–1483. https://doi.org/10.1158/1535-7163.MCT-08-1037/354637
23. Philoppes JN, Abdelgawad MA, Abourehab MAS, Sebak M, A. Darwish M, Lamie PF. Novel N-methylsulfonyl-indole derivatives: biological activity and COX-2/5-LOX inhibitory effect with improved gastro protective profile and reduced cardio vascular risks. *J Enzym Inhib Med Chem.* 2023;38:246–266. https://doi.org/10.1080/14756366.2022.2145283
24. Kryshchyshyn-Dylevych A, Radko L, Finiuk N, et al. Synthesis of novel indole-thiazolidinone hybrid structures as promising scaffold with anticancer potential. *Bioorg Med Chem.* 2021;50:116453. https://doi.org/10.1016/J.BMC.2021.116453
25. Sigalapalli DK, Pooladanda V, Singh P, et al. Discovery of certain benzyl/phenethyl thiazolidinone-indole hybrids as potential anti-proliferative agents: synthesis, molecular modeling and tubulin polymerization inhibition study. *Bioorg Chem.* 2019;92. https://doi.org/10.1016/J.BIOORG.2019.103188
26. Mushtaque M, Avecilla F, Azam A. Synthesis, characterization and structure optimization of a series of thiazolidinone derivatives as Entamoeba histolytica inhibitors. *Eur J Med Chem.* 2012;55:439–448. https://doi.org/10.1016/J.EJMECH.2012.06.052
27. Wang S, Zhao Y, Zhang G, Lv Y, Zhang N, Gong P. Design, synthesis and biological evaluation of novel 4-thiazolidinones containing indolin-2-one moiety as potential antitumor agent. *Eur J Med Chem.* 2011;46:3509–3518. https://doi.org/10.1016/J.EJMECH.2011.05.017
28. Pavlinac IB, Persoons L, Beč A, et al. Synthesis of novel imino-coumarin and acrylonitrile 2-benzazole hybrids as potent anticancer agents targeting tubulin. *Bioorg Chem.* 2025;154. https://doi.org/10.1016/j.bioorg.2024.107991
29. Salentin S, Schreiber S, Haupt VJ, Adasme MF, Schroeder M. PLIP: fully automated protein-ligand interaction profiler. *Nucleic Acids Res.* 2015;43:W443–W447. https://doi.org/10.1093/NAR/GKV315
30. Alpízar-Pedraza D, de la A, Veulens N, Araujo EC, Piloto-Ferrer J, Sánchez-Lamar Á. Microtubules destabilizing agents binding sites in tubulin. *J Mol Struct.* 2022;1259. https://doi.org/10.1016/J.MOLSTRUC.2022.132723
31. Bai R, Hamel E. (–)-Rhazinilam and the diphenylpyridazinone NSC 613241: two compounds inducing the formation of morphologically similar tubulin spirals but binding apparently to two distinct sites on tubulin. *Arch Biochem Biophys.* 2016;604:63–73. https://doi.org/10.1016/J.ABB.2016.06.008
32. Rai SS, Wolff J. Localization of the vinblastine-binding site on beta-tubulin. *J Biol Chem.* 1996;271:14707–14711. https://doi.org/10.1074/JBC.271.25.14707
33. Daina A, Michielin O, Zoete V. SwissADME: a free web tool to evaluate pharmacokinetics, drug-likeness and medicinal chemistry friendliness of small molecules. *Sci Rep.* 2017;7(1 7):1–13. https://doi.org/10.1038/srep42717